Characterisation of Group 4 Metallocenes and Metallocene Catalysts—UV/VIS Spectroscopic Study

Nora Mäkelä-Vaarne

Borealis Polymers Oy, R&D
Finland
&
Laboratory of Inorganic Chemistry
Faculty of Science
University of Helsinki
Finland

Academic Dissertation

To be presented, with the permission of the Faculty of Science of the University of Helsinki, for public criticism in Auditorium A129 of the Department of Chemistry, on October 10th, 2003 at 12 noon.

Helsinki 2003

ISBN 952–91–6252–9 (paperback)
ISBN 952–10–1318–4 (PDF)
Yliopistopaino
ethesis.helsinki.fi
Helsinki 2003

To Mika

Supervisor

Prof. Markku Leskelä
Laboratory of Inorganic Chemistry
Department of Chemistry
University of Helsinki
Finland

Reviewers

Docent Barbro Löfgren
Laboratory of Polymer Technology
Helsinki University of Technology
Finland

Prof. Reko Leino
Laboratory of Organic Chemistry
Åbo Akademi University
Finland

Opponent

Dr. Incoronata Tritto
Instituto per lo Studio delle Macromolecole del C.N.R.
Milano, Italy

Abstract

The performance of a group 4 metallocene based catalyst in olefin polymerisation is dictated by its active species. The electronic and steric structure, concentration, formation kinetics, stability and reactivity of the active species are the most important properties determining catalyst behaviour. Characterisation of these properties is a prerequisite for successful catalyst design and development.

The effect of structural and geometric factors on the electronic constructions of a group of zirconocenes was studied in detail by ultraviolet and visible (UV/VIS) spectroscopy in combination with theoretical calculations. The ligand to metal charge transfer (LMCT) absorption detected by UV/VIS spectroscopy is a measure of the energy difference between the ligand based highest occupied and the metal based lowest unoccupied molecular orbitals (HOMO–LUMO). The LMCT energy decreases as the electron donating ability of the ligand substituents and the electropositivity of the metal increase. Moreover, distortion of the complex geometry from the optimal metal–ligand bonding angles and orientation is detected as decreased LMCT energy.

UV/VIS spectroscopy and theoretical calculations were also used to study the effect of siloxy substituents attached to the zirconocene ligand framework on the catalyst activation by methylaluminoxane (MAO). The Zr–O(siloxy) and (MAO)Al–O(siloxy) interactions were found to be present, though the latter only at very high [Al]/[Zr] ratios. Furthermore, a catalyst activity–electronic structure relationship was established for a group of siloxy substituted zirconocenes: increasing catalyst activity correlated with decreasing LMCT energy.

UV/VIS spectroscopy in combination with extended X-ray absorption fine structure (EXAFS) measurements was employed to study the hafnium species present on a silica-supported hafnocene catalyst. The reaction of hafnocene with partially dehydroxylated silica was more efficient than its reaction with MAO-treated silica, the latter resulting in a wider variety of hafnocene species. The ratios of the species vary with the preparation technique.

Light exposure increases the activity of zirconocene catalyst in olefin polymerisation, especially in the presence of the catalyst poison oxygen. UV/VIS spectroscopy of the zirconocene/MAO/monomer system revealed that, when the catalytic system is exposed to light, the monomer–zirconocene interaction is favoured over the O_2–zirconocene interaction.

Preface

This work was carried out in the R&D laboratories of Borealis Polymers Oy in Porvoo during the years 1999–2003. The flexibility and support of Borealis and the funding from the Alfred Kordelin Foundation were of great assistance.

I am deeply grateful to my supervisor Prof. Markku Leskelä for his excellent advice and the many wise opinions that he shared with me. I am also most grateful to Prof. Hilkka Knuuttila who is largely responsible for the existence of this thesis. She took me on as a researcher at Borealis to work in the fascinating field of metallocene catalysis and early appreciated the possibilities of UV/VIS spectroscopy in metallocene catalyst research.

I have been privileged to work in excellent teams, first of all with Dr. Mikko Linnolahti and Prof. Tapani Pakkanen from the University of Joensuu. Three of the six publications on which this thesis is based are the result of this seamless co-operation. Scientific work was truly exciting with Dr. Astrid Lund Ramstad and Prof. David Nicholson (Norwegian University of Science and Technology), who allowed me to participate in the EXAFS measurements at the Swiss–Norwegian beamline, ESRF, France. It was a privilege to have enjoyed the co-operation of the most renowned person in the field of zirconocene catalysis, Prof. Hans-Herbert Brintzinger from the University of Konstanz. Finally, a special word of thanks to my wonderful colleague Mr. Kalle Kallio and his supervisor Prof. Karl-Heinz Reichert (Technische Universität Berlin) for introducing me to the captivating studies on light activation.

The innovative and cheerful working atmosphere in the R&D laboratories at Borealis has been an inspiration. In particular I would like to thank Dr. Sami Hietala for refreshing discussions; Dr. Tuulamari Helaja, Dr. Timo Laine and Ms. Marina Surakka for insightful comments on this work, and Ms. Paula Oinonen and the whole Analytical Services department for their great technical expertise.

Finally, warmest thanks go to my parents Antti and Pirkko Mäkelä for their firm belief in me, and to my husband Mika Vaarne for his continuous support and encouragement.

Helsinki, September 2003 Nora Mäkelä-Vaarne

Contents

List of original publications

This thesis is based on the following publications, which are referred to in the text by the Roman numerals I–VI:

I Mäkelä, N. I.; Knuuttila, H. R.; Linnolahti, M.; Pakkanen, T. A. Electronic transitions of racemic ethylene-bridged bis(indenyl)-type siloxy substituted zirconocene dichlorides. A combined UV/VIS spectroscopic and theoretical study. *J. Chem. Soc., Dalton Trans.*, **2001**, 91–95.

II Wieser, U.; Schaper, F.; Brintzinger, H-H.; Mäkelä, N. I.; Knuuttila, H. R.; Leskelä, M. Effects of an Interannular Bridge on Spectral and Electronic Properties of Bis(cyclopentadienyl)- and Bis(indenyl)zirconium(IV) Complexes. *Organometallics*, **2002**, *21*, 541–545.

III Mäkelä, N. I.; Knuuttila, H. R.; Linnolahti, M.; Pakkanen, T. A.; Leskelä, M. A.; Activation of Racemic Ethylene-Bridged Bis(indenyl)-Type Siloxy-Substituted Zirconocenes with Methylaluminoxane. A Combined UV/vis Spectroscopic and ab initio Hartree-Fock Study. *Macromolecules*, **2002**, *35*, 3395–3401.

IV Mäkelä-Vaarne, N. I.; Linnolahti, M.; Pakkanen, T. A.; Leskelä, M. A.; Role of Siloxy Substituents in the Activation of Zirconocene Polymerization Catalysts with Methylaluminoxane. A Combined Spectroscopic and Theoretical Study. *Macromolecules,* **2003**, *36*, 3854–3860.

V Mäkelä-Vaarne, N. I.; Nicholson, D. G.; Ramstad, A. L.; Supported metallocene catalysts—interactions of $(n\text{-BuCp})_2HfCl_2$ with methylaluminoxane and silica. *J. Mol. Catal. A: Chem.* **2003**, *200*, 323–332.

VI Mäkelä-Vaarne, N. I.; Kallio, K.; Reichert, K-H.; Leskelä, M. A.; Effect of Light Exposure on UV-Vis Spectrum of $[(n\text{BuCp})_2ZrCl_2]$ Based Catalyst. *Macromol. Chem. Phys.* **2003**, *204*, 1085–1089.

Author’s contribution to the publications

Publications **I**, **III** and **IV**

Nora Mäkelä-Vaarne drew up the research plan and wrote the manuscripts in close co-operation with Mikko Linnolahti. Nora Mäkelä-Vaarne was responsible for the experimental part and Mikko Linnolahti for the theoretical calculations.

Publication **II**

Nora Mäkelä-Vaarne provided the original idea and spectroscopic data for the publication and participated in the preparation of the manuscript.

Publication **V**

Nora Mäkelä-Vaarne drew up the research plan and wrote the manuscript in close co-operation with Astrid Lund Ramstad and David Nicholson. Nora Mäkelä-Vaarne was responsible for the UV/VIS spectroscopic part and Astrid Lund Ramstad and David Nicholson for the EXAFS calculations.

Publication **VI**

Nora Mäkelä-Vaarne drew up the research plan and wrote the manuscript in close co-operation with Kalle Kallio. Nora Mäkelä-Vaarne was responsible for the experimental part of the publication.

Abbreviations

UV/VIS	Ultraviolet and Visible
LMCT	Ligand to Metal Charge Transfer
HOMO	Highest Occupied Molecular Orbital
LUMO	Lowest Unoccupied Molecular Orbital
Cp	η^5-cyclopentadienyl ligand
Cp’	Any η^5-cyclopentadienyl based ligand
Ind	Indenyl ligand
Me	Methyl group
n-Bu	*n*-Butyl group
R	Alkyl group
TMA	Trimethylaluminium
MAO	Methylaluminoxane
NMR	Nuclear Magnetic Resonance
FTIR	Fourier Transform Infrared
XPS	X-ray Photoelectron Spectroscopy
EXAFS	Extended X-ray Absorption Fine Structure
HF	Hartree-Fock

1 Introduction

Group 4 metallocene catalysts exhibit high activities in olefin polymerisation and their single-site nature enables the synthesis of polymers with narrow molecular weight distributions and tailored microstructures. They offer a significant advantage over the conventional industrially used heterogeneous Ziegler-Natta and chromium oxide catalysts, the structures of which contain several different active sites making it difficult to control the polymer structure.[1]

1.1 Historical background

The first metallocene was discovered in 1951 in the form of ferrocene, $Fe(Cp)_2$.[2,3] The sandwich structure of ferrocene was formulated in 1952 by Wilkinson and Woodward[4] and a number of other metallocenes were established after this discovery.[5] Titanocene dichloride was found to be active in olefin polymerisation in 1957.[6,7] In these experiments aluminium alkyls were used as activators but only low polymerisation activities were obtained. It was not until 1973 that the true potential of group 4 metallocene catalysts was recognised—it was observed that controlled addition of water into the titanocene/aluminium alkyl system raises the catalytic activity dramatically.[8] The increase in activity was found to arise from the formation of aluminoxanes, *e.g.* methylaluminoxane (MAO) from the reaction of trimethylaluminium (TMA) and water.[9] Many research groups proceeded to develop new metallocene complexes once the potential of metallocenes was established. One major advance was the synthesis of bridged zirconocene dichlorides with C_2 symmetry by Brintzinger in 1985.[10] Soon after this, Kaminsky and co-workers produced isotactic polypropylene with these bridged zirconocenes.[11] Their success spurred efforts to find more active and stereoselective catalysts for the polymerisation of a wide range of monomers.[12] Still today, MAO-activated metallocene catalysts are a subject of extensive research.[11,13] Although group 4 metallocene based catalysts are already being employed in the polyolefin industry[14], much work remains to be done in the field of catalyst design to widen the property window of the resulting polymer.

1.2 General structure of group 4 metallocenes

The general structure of a group 4 metallocene catalyst precursor such as used in olefin polymerisation is presented in Fig. 1. In the Cp'_2MXY complex shown, the central metal, M, is Zr (IV), Hf (IV) or Ti (IV) and the leaving groups, X and Y, are usually Cl or CH_3. The η^5-bonded "tilted sandwich" cyclopentadienyl (Cp) ligands can be substituted and can be connected by an interannular bridge (Cp'). The metallocene structure described in Fig. 1 is a tetrahedral 16-electron complex with unoccupied metal *d*-orbitals (d^0). One of the five *d*-orbitals of M is left vacant.[15]

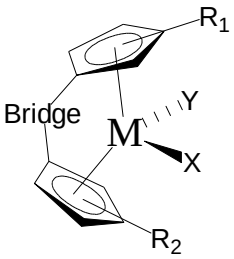

Figure 1. General structure of a bridged group 4 metallocene catalyst precursor.

The bridge structure restricts the Cp' ligands from free rotation. Despite the resticted movement, ethylene bridged bis(indenyl) complexes are flexible enough to exist in two extreme conformations, forward and backward. Both forward and backward conformations, as well as the conformations between them, are present in solution if the interconversion barrier is low enough (Fig. 2). In ethylene bridged bis(indenyl) zirconocenes indenyl-forward conformations are generally slightly favoured.[16]

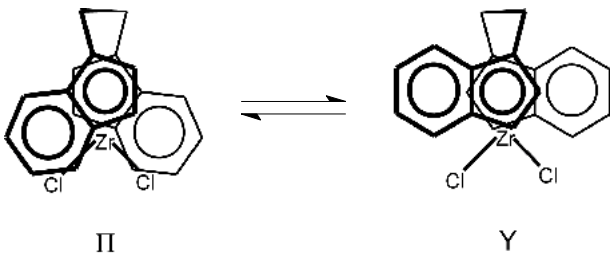

Figure 2. Top view of indenyl-forward (Π) and indenyl-backward (Y) conformations.[I]

1.3. Activation of group 4 metallocenes

Group 4 metallocene complexes need to be activated before being used in olefin polymerisation.[17] The activator should be able to alkylate the metallocene. In some cases this need can be circumvented by using metallocene dialkyls as catalyst precursors. Other commonly accepted prerequisites for the activator are that it should be able to intake X and Y leaving groups (Fig. 1) and act as an only weakly co-ordinating counterion, so that it does not hinder the olefin co-ordination to the cationic metal centre. Further, the activator should be capable of reactivating the deactivated species (Scheme 1). MAO fulfils all the preceding requirements and is the most commonly used activator for metallocene catalysts. In addition, MAO acts as a scavenger of catalyst poisons by reacting with impurities such as oxygen and water that may be present in the catalytic system. Though intensively investigated, the structure of MAO is only partly resolved. Generally, it consists of oligomeric –$Al(CH_3)$–O– structural units and complexed trimethylaluminium residues forming cage structures that are in dynamic equilibrium with each other.[18] MAO is needed in large excess; [Al]/[M] ratios of 200–5000 are often used for metallocene activation. The reasons for the required excess are still not fully clarified.[18]

It is well documented that group 4 metallocene cations are responsible for the catalyst activity in olefin polymerisation. The formation of a 14-electron complex, $[Cp'_2ZrMe]^+$, in the presence of MAO has been detected by X-ray photoelectron spectroscopy (XPS)[19] as well as by ^{13}C and ^{91}Zr nuclear magnetic resonance (NMR)[20,21] spectroscopic techniques. The presence of cationic metallocene species has also been verified by the use of weakly co-ordinating anions, such as $(C_6H_5)_4B^-$ and $(C_6F_5)_4B^-$, as counterions for alkylated metallocene cations.[22] Methylation reaction takes place before cationisation, and the methylation step has been studied by UV/VIS[23,24,III] and ^1H and ^{13}C NMR[25–29] spectroscopy. These studies have suggested the formation of a monomethylated species for a metallocene/MAO complex at low [Al]/[Zr] ratios of 10–20.

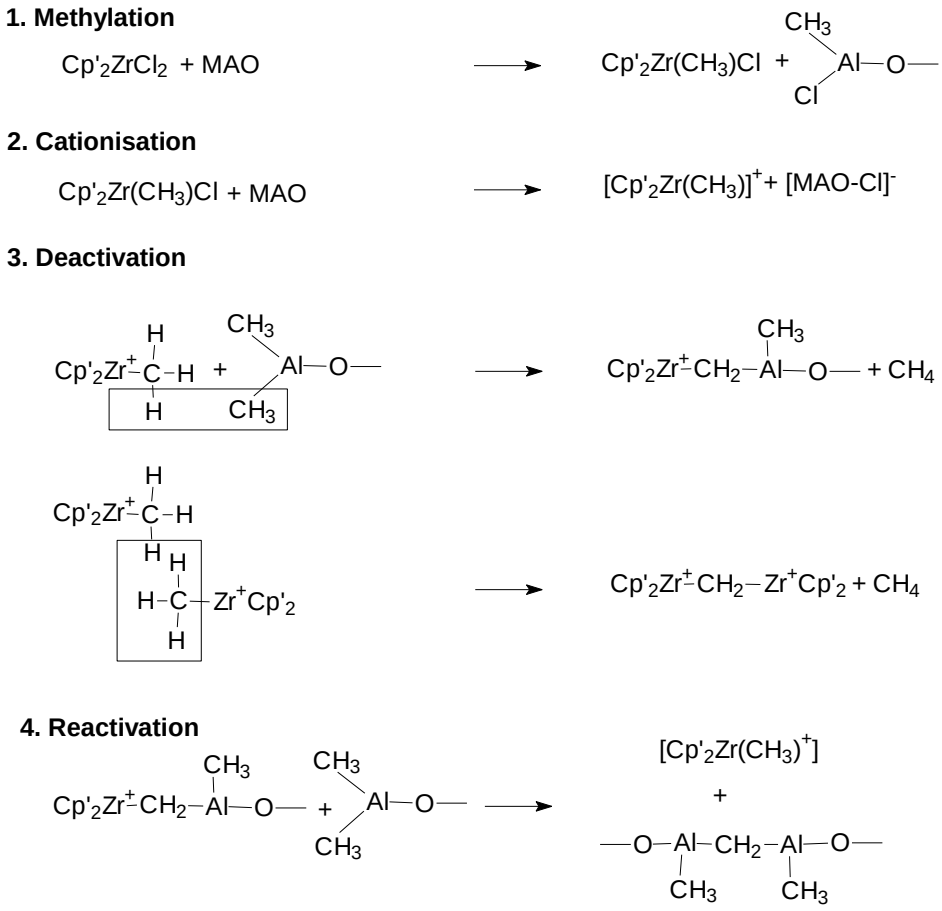

Scheme 1. Reactions of group 4 metallocene with MAO. Zirconocene dichloride is presented as an example.[13,30,31]

As described in Scheme 1, deactivation of zirconocene catalyst in a pure zirconocene/MAO system occurs via methane abstraction through formation of a Zr–CH_2–Al bimetallic species. Fortunately, the deactivated bimetallic species can be reactivated by MAO through ligand exchange. This lengthens the lifetime of the catalyst in polymerisation.[31] A similar α-hydrogen elimination with formation of methane and still slightly active Zr–μ–CH_2–Zr complexes was demonstrated by Bochmann *et al.*[32] for cationic zirconium alkyl catalysts. Catalyst deactivation can also occur if a Lewis basic compound such as oxygen or water is present. The Lewis basic compound co-ordinates to and reacts with the Lewis acidic metal centre, which then becomes inactive for olefin polymerisation.

1.4 Polymerisation mechanism models

Three main models for olefin co-ordination polymerisation have been suggested: 1) the direct insertion model proposed by Cossee and Arlman,[33] which involves monomer co-ordination to the electrophilic, co-ordinatively unsaturated cationic complex, followed by monomer insertion into the metal–alkyl bond to extend the polymer chain; 2) the methathesis model proposed by Green and Rooney,[34] in which an α-hydrogen is transferred from the end of the polymer chain to the metal, leading to a metal carbene complex, which together with the co-ordinated monomer forms a metallacyclobutane complex via which the monomer inserts to the polymer chain; 3) the modified Green–Rooney model proposed by Brookhart and Green,[35] in which insertion proceeds via migration of the polymer chain to the olefin ligand and is suggested to occur through a four-centre transition state, stabilised by agostic interactions between the metal centre and an α-hydrogen of the growing chain (Scheme 2).[35,36]

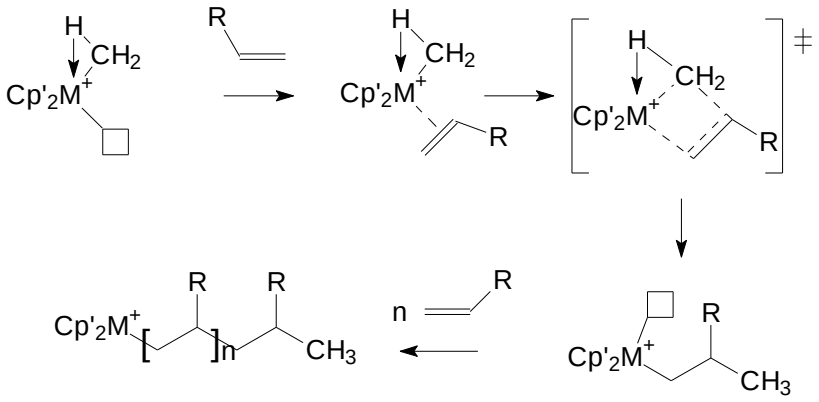

Scheme 2. A model for olefin co-ordination polymerisation (modified Green–Rooney) constructed by Brookhart *et al.*[35] from the Cossee–Arlman[33] and Green–Rooney[34] models. The activator is omitted for clarity, Cp'=Cp based ligand, R=H or CH_3.

The polymerisation continues until termination of the polymer chain growth takes place. Chain termination may occur by β-H elimination to the metal, by β-H

elimination to a co-ordinated monomer, by chain transfer to aluminium or most likely by chain transfer to hydrogen, if hydrogen is present.[13,30]

1.5 Influence of the metallocene structure

As described earlier for Cp'$_2$MXY (Fig. 1), group 4 metallocene catalyst precursors typically have unoccupied metal *d*-orbitals. This is important since the probability of β-H elimination in the polymerisation reaction, leading to unwanted oligomerisation, is lower when lone electron pairs are not available.[37] Substituents attached to the Cp' rings influence the catalyst behaviour markedly, by electronic or steric effects. Moreover, fine adjustment of the M–X or M–Y bond stability is possible through variation of the electronic effects of the Cp' ligands. The stability of these bonds is important since catalyst activation is easier if the bonds are weaker. Unstable M–alkyl bond also facilitates olefin insertion and thus increases catalyst activity. Electron-donating substituents in the Cp' ligand framework are generally assumed to increase the catalyst activity. The better electron donor the Cp' ligand, the lower is the positive charge of the metal. As a consequence, the bonding between the metal and the X and Y ligands will be weaker and the reactivity of the M–X and M–Y bonds will be enhanced.[30] Electron withdrawing substituents have the reverse effect as they complicate the activation of the catalyst precursor.[38] Bulky ligands can hinder monomer co-ordination to the active centre by filling the space around the active centre and thus they decrease the catalyst activity in olefin polymerisation.[39] The bridge structure restricts the rotation of the Cp' ligands improving the stereospecificity of polymerisation, and it expands the space between the two Cp' ligands where the polymerisation reaction takes place.[40]

1.6 Scope of the thesis

This thesis summarises studies on the electronic structure of zirconocenes and characterisation studies on both supported and unsupported group 4 metallocene catalysts. Intermediate species in the activation reaction were also of interest. The

techniques employed were UV/VIS spectroscopy in combination with theoretical calculations,[I,II,III,IV] olefin polymerisation[III,VI] and EXAFS spectroscopy.[V]

In the first part of the thesis, relationships between the chemical, steric and electronic structures of zirconocenes were established by applying UV/VIS spectroscopy and theoretical calculations.[I,II] The information obtained was used as a basis for interpreting the UV/VIS absorptions of activated catalysts.[III,IV] As a means to extending the applications of UV/VIS spectroscopy, a correlation was sought between the electronic structure of a group of zirconocene catalysts and their polymerisation activity.[III] Siloxy substituted zirconocenes[41] give highly active catalysts for olefin polymerisation.[42–45] The reasons for this high activity and the effect of the siloxy substituent on the activation behaviour of zirconocene catalyst were discussed.[III,IV] Also, UV/VIS spectroscopy together with EXAFS was used to characterise silica-supported hafnocene catalysts.[V] Finally, the effect of light irradiation and catalyst poison oxygen on the zirconocene catalyst reactivity with an olefin monomer was investigated by UV/VIS spectroscopy.[VI] Scheme 3 presents the group 4 metallocene catalyst precursors used in the studies summarised in this thesis.

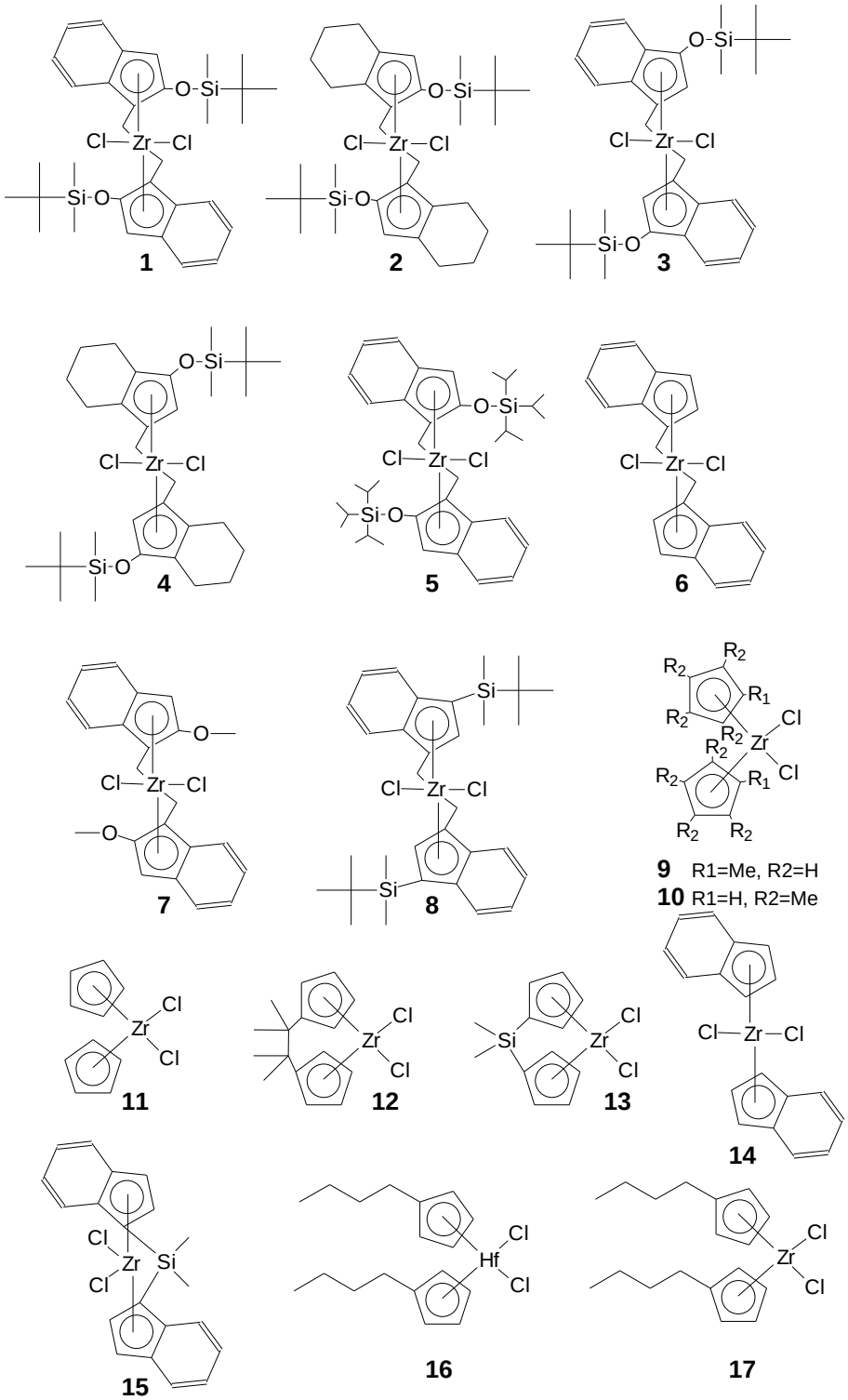

Scheme 3. Schematic structures of the group 4 metallocene catalyst precursors studied in this work.

2 Characterisation of unsupported group 4 metallocene catalysts

2.1 General requirements

Several requirements apply in the characterisation of unsupported group 4 metallocene catalysts. Metallocene catalysts, consisting of a group 4 metallocene complex and MAO, are reactive towards Lewis acids and thus measurements must be performed under an inert atmosphere and in dry solvents. The concentrations of the complex of interest should be at the same level in the analytical measurement as in the actual polymerisation, *i.e*. rather low. In addition, variable amounts of MAO, *e.g.* [Al]/[M]=1–10000, should be used, depending on the purpose of the study. In-situ monitoring is a special requirement for studies on catalyst activation, monomer reaction and catalyst deactivation. If the effect of the support on the catalyst is of interest, as it was in this work, it is advantageous to be able to use the same technique for supported and unsupported samples. Taking into account the special requirements described above, a limited number of techniques are suitable for metallocene catalyst characterisation.

2.2 Earlier studies

The major findings of the most relevant studies on homogeneous group 4 metallocene catalyst and catalyst precursor characterisation, excluding polymerisation and UV/VIS spectroscopic studies, are summarised in the following. UV/VIS spectroscopic studies are reviewed in section 3.1.2 and studies dealing with supported catalysts in section 7.1.

Gassman *et al.*[46,47] have studied the binding energies in zirconocenes and hafnocenes by X-ray photoelectron spectroscopy (XPS). The zirconium and hafnium 3*d* binding energy was found to decrease systematically with increasing methyl substitution of the Cp ring,[46,47] decreasing the Zr 3*d* binding energy value and leading to increasing catalyst polymerisation activity[48]. XPS has also been used to study the interaction of

MAO and zirconocenes.[19,49] Formation of a cationic complex upon MAO addition was concluded from the noticeable increase in the zirconium binding energy. Addition of ethylene to the zirconocene/MAO system decreased the binding energy, evidently through reaction of ethylene with the Zr centre.[19]

Electronic and steric effects of a group of Cp' ligand substituents on the activity of $(CpR)_2ZrCl_2$/ethylaluminoxane were quantified by Möhring and Coville[50] using a combination of zirconocenes' geometrical data and electronic parameters of the ligands. It was concluded that the activity of the catalytic system increases with size of the R substituents as well as with their electron donating ability.

The tendency of a zirconocene complex to exchange a chloride for a methyl group has been reported to be a measure of the electron deficiency at its Zr centre.[51,52] This was shown by determining the equilibrium constants of the exchange reaction by ^{1}H NMR spectroscopy. The fact that uptake of a methyl group is favoured by decreased electron density at the zirconium centre of a zirconocene dichloride complex means that zirconocenes with Cp' ligands that are effectively electron donating will have a less cationic zirconium centre and a slower methylation process.

Tritto and co-workers[27,28] have extensively studied the reactions of zirconocenes and titanocenes with MAO, TMA and $B(C_6F_5)_3$ using ^{1}H and ^{13}C NMR spectroscopy. The experiments were performed at temperatures from 203 K to 283 K with [Al]/[M] ratios 1–40 and Zr or Ti concentrations of 0.01–0.07 mol/dm^3. For the zirconocene/MAO system, evidence was found for the formation of monomeric $[Cp_2Zr(^{13}CH_3)]^+$, dimeric $[Cp_2Zr(^{13}CH_3)]_2(\mu\text{–}CH_3)^+$ and small amounts of methyl-bridged $[Cp_2Zr(\mu\text{–}CH_3)_2Al(CH_3)_2]^+$ cationic species with $[CH_3(MAO)]^-$ counterions.[28] Increased temperature and [Al]/[M] ratio and decreased Zr concentration were observed to shift the equilibrium towards monomeric $[Cp_2Zr(^{13}CH_3)]^+$.[28] Earlier the binuclear species have been assigned as possible dormant states for the active sites[29] as well as being hypothesised to be the active species in ethylene polymerisation.[53] To clarify this, Babushkin *et al*. extended the range of [Al]/[Zr] ratios studied by ^{1}H and ^{13}C NMR spectroscopy to 10–4000 and zirconocene concentrations were reduced down to 0.0005 mol/dm^3.[54] The authors proposed three cationic zirconocene

intermediates, of which the active species was dimeric $[Cp_2Zr(\mu–CH_3)_2Al(CH_3)_2]^+$ $[CH_3(MAO)]^-$, and the dormant species was monomeric $[Cp_2Zr(CH_3)]^+$ $[CH_3(MAO)]^-$. The structures of these active and dormant sites were supported by density functional theory calculations of Zurek and Ziegler.[55]

3 Research methods of this study

The main research technique used in the investigations was UV/VIS spectroscopy. The UV/VIS spectroscopic studies were supported by theoretical calculations, EXAFS analysis and polymerisation tests.

3.1 UV/VIS Spectroscopy

Ultraviolet and visible (UV/VIS) spectroscopy measures transitions between the electronic energy levels of a molecule. The transitions in an organic compound generally occur between a bonding or a lone-pair orbital and an unoccupied non-bonding or anti-bonding orbital. In organometallic complexes, ligand to metal charge transfer (LMCT) can occur as well. In LMCT, electron density is transferred from the ligand orbitals to the metal orbitals. If only transitions between the electron energy levels were involved, the UV/VIS spectra of all compounds would consist of fairly sharp lines. Instead of sharp peaks, however, smooth curves are recorded, because any change in the electronic energy is accompanied by a corresponding change in the rotational and vibrational energy levels, and interactions of solute molecules with the solvent blur out the rotational and vibrational fine structure.[56]

3.1.1 Limitations and advantages of the technique

A UV/VIS spectrum does not give detailed qualitative information on the structures of the species present in the sample and a complementary technique is required for that purpose. Quartz cells can withstand only fairly low pressures, <1 bar, limiting the possibilities to duplicate high pressure polymerisation conditions. The repeatability of

the analysis depends on the accuracy of weighing and diluting the samples. The advantages of UV/VIS spectroscopy were considered to outweigh the disadvantages, however, and UV/VIS spectroscopy was chosen as main research technique. UV/VIS measurements can be performed under inert gas in dry hydrocarbon solvents. Concentrations of metallocene complex as low as in polymerisations can be measured, and high excess of MAO does not disturb the interpretation of the spectrum since it does not absorb in the same range as the most relevant LMCT transitions of group 4 metallocenes. Sampling is easy, and in-situ measurements are fast and can be performed at various temperatures. Supported catalysts can be studied with the aid of a diffuse reflectance accessory, and the recorded reflectance can be translated to correlate with absorbance measurements.[V,VI] In addition, UV/VIS spectrometers are basic, relatively low price instruments and thus widely available in laboratories.

3.1.2 UV/VIS spectroscopy in group 4 metallocene catalyst research

In this UV/VIS spectroscopic study on group 4 metallocene complexes and their activation, the most interesting absorptions were LMCT transitions. These transitions occur because the ligands are electron rich and the metal is electron poor. For these same reasons, neither metal to ligand charge transfer (MLCT) nor *d–d* transitions occur, so that the spectral interpretation is simplified. Other possible transitions besides LMCT occur within the aromatic ligand and between a heteroatom substituent and aromatic ligand. Fortunately, these absorptions generally take place in the ultraviolet range, while the LMCT transitions occur mainly in the visible range of the electromagnetic spectrum.[56]

Fig. 3 presents a typical UV/VIS spectrum of a zirconocene dichloride. The band with maximum at 385 nm is the charge transfer transition from indenyl ligand to Zr metal, *i.e.* Ind→Zr LMCT transition.[I] The UV absorption range up to 320 nm consists of the Cl→Zr LMCT and the other above-mentioned absorptions.

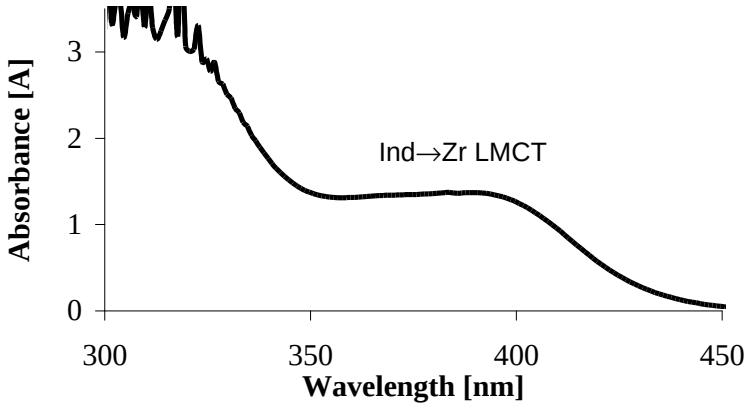

Figure 3. UV/VIS spectrum of $(Ind)_2ZrCl_2$ (**14**) in toluene solution.

Zirconocene activation with MAO can be studied by UV/VIS spectroscopy.[23,24,57] Two successive LMCT band shifts have been detected for the **1**/MAO catalyst system with increasing [Al]/[Zr] ratio[III] (Fig. 4): 1) an LMCT band shift to higher energies at [Al]/[Zr]<30 (hypsochromic shift) and 2) a shift to lower energies with increasing [Al]/[Zr] ratio up to 7500 (bathochromic shift). These two shifts can be understood as produced by methylation and cationisation of the zirconocene, respectively.

The replacement of the chlorides with more electron-donating methyl groups results in an increase in the electron density at the central zirconium metal. As a result, more energy is needed to push the electrons from the Cp' ligand to Zr and an LMCT band shift to higher energies, *i.e.* to shorter wavelengths, is detected.[23] This LMCT shift has been concluded to arise from monomethylation rather than dimethylation of the zirconocene dichloride complex.[24,III] This is demonstrated in Fig. 4, where the LMCT band of the zirconocene reacted with MAO, [Al]/[Zr]=20, is located halfway between the LMCT bands of the corresponding dimethyl and dichloride complexes. The bathochromic shift at higher [Al]/[Zr] ratios was concluded to be an indication of cation formation.[23] Zirconocene is cationised so that it is left with one methyl group and a positive charge in addition to the two Cp' ligands. The charge transfer from Cp' to electron poor Zr therefore requires less energy, and an LMCT band shift to lower energies, *i.e.* to longer wavelengths, is observed.

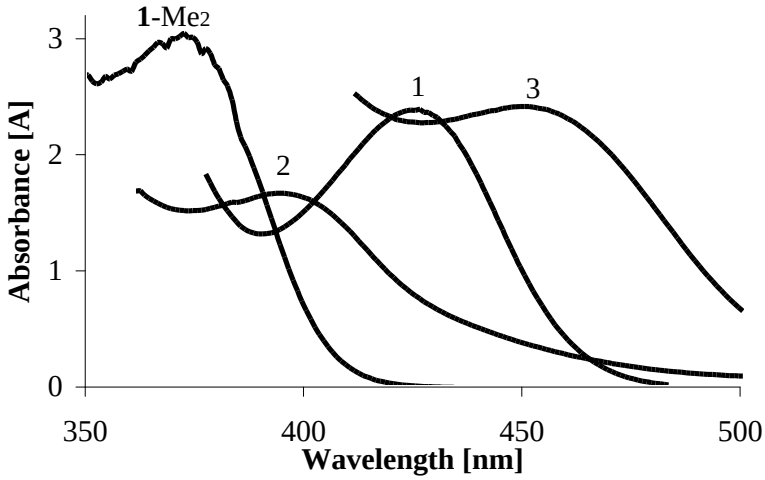

Figure 4. The lowest energy LMCT absorptions of complex **1:** 1) in toluene, 2) methylated with MAO ([Al]/[Zr]=20) and 3) cationised with MAO ([Al]/[Zr]=1000). Dimethylated complex **1** in toluene is included as a reference.[III]

Three successive LMCT band shifts with increasing [Al]/[Zr] ratios have been reported for $Et(Ind)_2ZrCl_2$/MAO[23] and $Me_2Si(Ind)_2ZrCl_2$/MAO[58]. The first shift was assigned as described above, while the second shift was suggested to arise from associated cationic zirconocene species. The third shift was concluded to indicate cation dissociation, *i.e* increased positive charge for zirconium (Fig. 5). The first shift for these complexes was detected at [Al]/[Zr]<30, as for complex **1**/MAO. The second shift for these complexes was observed in the [Al]/[Zr] range of 30–200 and the third bathochromic shift at higher ratios ([Al]/[Zr]=200–2000).[23]

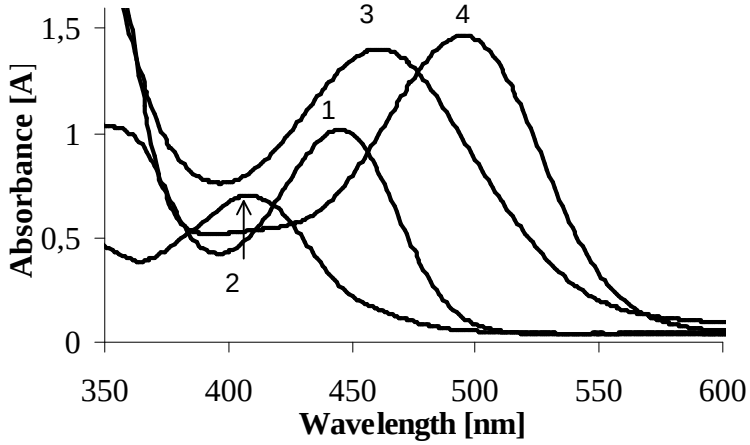

Figure 5. Activation behaviour of $Me_2Si(Ind)_2ZrCl_2$ (complex **15**)/MAO: 1) [Al]/[Zr]=0; 2) [Al]/[Zr]=20, assigned to $Me_2Si(Ind)_2Zr(Me)Cl$; 3) [Al]/[Zr]=200, assigned to $Me_2Si(Ind)_2Zr(Me)^+$ associated; and 4) [Al]/[Zr]=1000, assigned to $Me_2Si(Ind)_2Zr(Me)^+$ dissociated. Four hours reaction in toluene.

UV/VIS studies on the catalytic system $Et(Ind)_2ZrCl_2$/MAO have revealed that the use of TMA-depleted MAO makes it possible to activate zirconocene at rather low [Al]/[Zr] ratios of 50–200. This emphasises the deactivating role of TMA when it is included in MAO.[59] Also, the chlorides of $Et(Ind)_2ZrCl_2$ that are attached to MAO in the activation process have been reported to negatively affect the catalyst activity.[60] This combined UV/VIS spectroscopic and 1-hexene polymerisation study revealed a strong $[MAO(Cl)]^-$ interaction with the vacant site of zirconocene cation, which impedes olefin co-ordination and insertion.[60] This finding was made for [Al]/[Zr]=150; at higher ratios ([Al]/[Zr]>500) the cationic species generated by MAO from various starting complexes were found to be independent of the nature of the abstracted leaving group.[61]

3.1.3 Experimental

For the UV/VIS measurements of unsupported catalysts, metallocene catalyst precursors and metallocene/MAO catalysts were dissolved in toluene and sealed in airtight one-centimetre path length quartz cells with Teflon® stoppers under dry nitrogen atmosphere. Supported catalyst samples were sealed in similar cells as such. The appropriate concentration of the dissolved complex was found to be about 8×10^{-4}

mol/dm^3. The spectra of the dissolved samples were collected with a Cary 50 Varian, Perkin Elmer Lambda 11 or Lambda 900 UV/VIS spectrophotometer in the wavelength range of 200–800 nm at ambient temperature. The spectrum scanning of the powder samples was performed in the same wavelength range and at the same temperature as the dissolved samples with a Perkin Elmer Lambda 900 UV/VIS spectrophotometer equipped with a Labsphere 60-mm integrating sphere. In the integrating sphere incident beam strikes the sample and the diffusely, *i.e.* with equal intensity to all directions, reflected radiation is collected by the sphere and, after repeated reflections, recorded at the detector. The inner coating of the sphere consists of a highly reflecting material, in this case Spectralon® from Labsphere. The measurements were carried out with reference to a Spectralon® sample. Translation of the reflectance spectrum to the corresponding absorption spectrum requires calculation with equation $A \approx \log(1/R)$. This is analogous to the equation used for changing transmittance to absorbance in the case of liquid samples: $A = \log(1/T)$.[56]

3.2 Theoretical calculations

Theoretical calculations were used as an aid in the interpretation of the UV/VIS spectroscopic results. Quantum chemical Hartree–Fock[I,III,IV] and semi-empirical Hückel molecular orbital[II] calculations were employed. Two factors limit the use of Hartree–Fock quantum chemical calculations for transition metal complexes: near-degeneracy and relativistic effects. Near-degeneracy effects originate from the fractional occupation of the *d*-shells, which gives rise to close-lying electronic states. Different sizes of the valence shell *s*- and *d*-orbitals aggravate the near-degeneracy problem due to non-optimal overlap between metal and ligand orbitals. The near-degeneracy effects are least significant for the second and third transition row complexes since their valence shell *s*- and *d*-orbital sizes are more similar.[62] Relativistic effects, on the other hand, are strongest for the third row elements, due to the high nuclear charge. Zirconium is located on the left side of the second row of transition elements, which means that neither near-degeneracy nor relativistic effects are too strong for the zirconocene complexes to be studied by quantum chemical Hartree–Fock method.

Hartree–Fock HF/3–21G* method is the optimal choice for geometry prediction for bridged zirconocene dichlorides.[63] The method produces rational structures consistent with the experimentally determined ones in reasonable calculation time. Also the extended Hückel molecular orbital method can reproduce angular overlap changes fairly reliably despite its shortcomings due to the semi-empirical basis.[64]

3.3 EXAFS

Extended X-ray absorption fine structure (EXAFS) spectroscopy is a versatile method for studying the structures of a uniform amorphous bulk material. The technique is based on the absorption of X-rays and the generation of photoelectrons, which are scattered by atoms nearby in the lattice. The interference effects, visible in the X-ray absorption spectrum, give detailed information about the distance, type and number of nearest and next nearest neighbours of the atoms of interest. The detection distance between the studied atom and the scatterer can be up to 6 Å in highly ordered crystalline systems. The amplitude of EXAFS oscillations increases with the co-ordination and atomic number of neighbours, while the frequency of oscillations depends inversely on interatomic distances, and the step height of the absorption edge is proportional to the concentration the atoms of interest in the sample. The high [Al]/[M] ratio in metallocene catalysts is not a problem in EXAFS since the method detects the surroundings of the selected metal, in metallocenes most interestingly the central metal. Relatively low Zr and Hf concentrations can be detected, and the sample preparation and measurements can be performed under inert gas. Unfortunately, the EXAFS data analysis is complicated and not always without ambiguity. Also the synchrotrons needed in collecting EXAFS data of highly disordered materials and of low concentration are not readily available. For these reasons EXAFS has not been widely used in the field of catalyst research.[65]

In this work EXAFS was applied to characterise the species existing in a hafnocene catalyst supported on partially dehydroxylated, porous silica.[V] The analysed samples, which consisted of a mixture of chemicals in very low concentrations on a porous silica powder, are not easily examined by most structural characterisation methods.

3.4 Polymerisation tests

Ethylene polymerisations were performed to determine the activity of the catalysts. The polymerisations were carried out as slurry polymerisations in pentane using homogeneous catalysts and 1-hexene as a comonomer.[III] Slurry co-polymerisation was selected since it is the standard polymerisation test method for homogeneous catalysts in the R&D laboratories of Borealis Polymers Oy, Porvoo.

4 Factors affecting the electronic structure of metallocenes

Catalyst properties can be divided into two equally important groups: steric and electronic. Steric effects of substituents and bridging units on the activity and stereoselectivity of zirconocene dichloride based polymerisation catalysts have been studied extensively.[13,66] The electronic effects of different ring substituents and central metals have also been studied, but not as thoroughly.[50,67] One major challenge is to differentiate these two simultaneously acting and interlinked effects. Variations in the steric structure often result in changes in electronic properties.

In this work, a group of metallocene dichlorides were studied by UV/VIS spectroscopy to find out how changes in the complex structures affect the electronic properties. It is plausible that such a relationship can be revealed by UV/VIS spectroscopy since the lowest energy LMCT transition detected by UV/VIS spectroscopy is a measure of the energy gap between the highest occupied and lowest unoccupied molecular orbitals (HOMO–LUMO). Theoretical calculations showed that, in the studied zirconocene complexes, the HOMO is Cp’ ligand based, while the LUMO is mainly of zirconium character.[II,III] Changes at the central metal and at the ligands are thus reflected in the LMCT energy. As well, the Cp’ ligand orientation and the bonding angles within the complex have a marked effect on the LMCT energies. These factors are discussed in sections 4.1–4.4.

4.1 Metal centre

A change in the metal centre of a group 4 metallocene becomes reflected in the LMCT energy. As noted earlier, the LUMO is based on the empty *d*-orbitals of the metal. When zirconium is replaced with another metal of group 4, hafnium or titanium, changes will occur in the LMCT energy. As can be seen in Fig. 6, hafnocene dichloride absorbs at higher and titanocene dichloride at lower energy.[68] When the metal forms more stable bonds with the Cp' ligands, the LMCT requires more energy. The bond angles in the metallocene do not change appreciably when zirconium is replaced by hafnium, which is almost the same size. For example, in $Cp_2Zr(CH_3)_2$ the CH_3–Zr–CH_3 bond angle is 95.6° and the Cp–Zr–Cp angle 132.5°, while for $Cp_2Hf(CH_3)_2$ these angles are 95.8° and 133.0°, respectively.[69] It can be assumed, therefore, that these minor changes in the bond angles do not significantly affect the LMCT absorption energies.

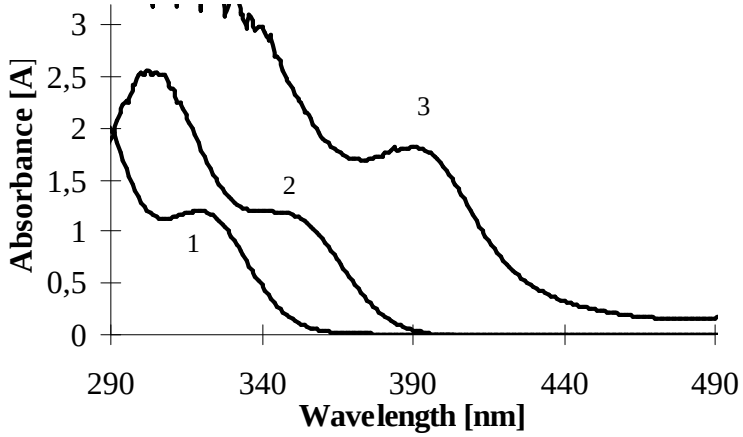

Figure 6. Effect of metal on LMCT transition energy. The UV/VIS spectra of 1) (*n*-BuCp)$_2$HfCl$_2$ (315 nm), 2) (*n*-BuCp)$_2$ZrCl$_2$ (339 nm) and 3) (*n*-BuCp)$_2$TiCl$_2$ (392 nm) in toluene.[68]

The electron deficiency of the metal, and therefore the energy of the LUMO orbital, may also be controlled by the substituents attached to the Cp' ligands. As the oxygen atom of the siloxy substituent in complexes **1**–**5** approaches the zirconium centre, it destabilises the LUMO by donating electron density towards it. The destabilisation effect is greater when the oxygen is able to bend closer to zirconium.[I] In the following

sections, the effect of other factors than the metal centre on LMCT is elucidated by focusing on zirconocenes.

4.2 Cp' ligand substitution

The effect of Cp' ligand substitution on the LMCT transition energy is not straightforward. Substitution of the Cp ligand in Cp_2ZrCl_2 with methyl groups was observed to decrease the energy of the LMCT absorption by about 4 nm for each pair of methyl groups (Table 1).[II] Electron donating methyl groups evidently destabilise the HOMO, which leads to a decreased HOMO–LUMO energy gap and thus lower LMCT energy. Since the LMCT absorption in question is a Cp'→Zr charge transfer, the LMCT energy might seem to be a measure of the electron donating ability of the Cp' ligand.

Table 1. Longest wavelength absorption bands of methyl substituted zirconocene dichlorides in toluene.[II]

Complex	λ **(nm)**	Δλ **(nm)**
Cp_2ZrCl_2 (**11**)	333	
$(MeCp)_2ZrCl_2$ (**9**)	337	4[a]
$(Me_4Cp)_2ZrCl_2$ (**10**)	350	17[a]

[a] Relative to $(Cp)_2ZrCl_2$,

UV/VIS spectroscopy alone is not, however, always an adequate tool to study electron donating abilities of different Cp' ligand substituents. Nearly identical complexes with only the position of the substituent changed absorb at different energies, namely complexes **1** *vs.* **3** and **2** *vs.* **4**. Moreover, the addition of $(CH_2)_2$ or Me_2Si bridge to a bis-indenyl zirconocene dichloride (**14** *vs.* **6** and **15**) results in a large bathochromic shift. These observations led us to study how changes in the complex geometry affect the LMCT energy.

4.3 Interannular bridge

As revealed in the previous section, interconnection of the indenyl ligands in bis(indenyl)zirconium dichloride zirconocenes by a 1,1´ positioned $(CH_2)_2$ or Me_2Si bridge causes pronounced bathochromic shifts of the longest wavelength UV/VIS absorption bands. These shifts are in the range of 41–59 nm. Adding a bridge structure to analogous bis(cyclopentadienyl) complexes results in much smaller shifts of 12–23 nm (Table 2). Clearly, then, the shift is not an effect due solely to the electron donating ability of the bridge unit since the extent of the LMCT band shift differs in indenyl and cyclopentadienyl based complexes.

Table 2. Longest wavelength LMCT absorption bands of bridged and unbridged zirconocene dichlorides in toluene.[II]

Complex	l **(nm)**	Dl **(nm)**
$(Cp)_2ZrCl_2$ (**11**)	333	
$Me_4C_2(Cp)_2ZrCl_2$ (**12**)	345	12[a]
$Me_2Si(Cp)_2ZrCl_2$ (**13**)	356	23[a]
$(Ind)_2ZrCl_2$ (**14**)	385	
$Et(Ind)_2ZrCl_2$ (**6**)	426	41[b]
$Me_2Si(Ind)_2ZrCl_2$ (**15**)	444	59[b]

[a] Relative to $(Cp)_2ZrCl_2$, [b] Relative to $(Ind)_2ZrCl_2$.

Since conformation and energy were suspected of being interrelated, theoretical calculations were performed to study the effects of changes in ligand conformation on the LMCT energy (Fig. 7). Rather large changes in the HOMO–LUMO energy gap were found to be associated with a change in orientation, especially in the case of bis(indenyl)-type zirconocene dichlorides. The HOMO, which is mainly indenyl based, is destabilised when the rotation of the indenyl ligands towards backward orientation reduces the overlap between the filled indenyl π and empty zirconium *d*-orbitals due to a mismatch of their nodal planes. The LUMO, dominated by the empty *d*-orbitals of zirconium, is less affected by the changes in the ligand orientation because it is nonbonding with regard to the indenyl ligands. When the torsion angle,

ϕ, increases from 55° (found in $(Ind)_2ZrCl_2$[70]) to 150° (found in $Me_2Si(Ind)_2ZrCl_2$[71]), the HOMO–LUMO energy gap decreases by 0.16 eV (Fig. 7). Increased ϕ-values thus appear to be responsible for the strong bathochromic shift of the longest wavelength LMCT absorption that is observed when a bridge structure forces the indenyl ligands into a more forward orientation.

Fig. 7 also reveals that in $(Cp)_2ZrCl_2$ (**11**) the HOMO–LUMO energy gap decreases by only 0.05 eV when the torsional angle ϕ changes from the staggered energy minimum to the eclipsed conformation found in $Me_2Si(Cp)_2ZrCl_2$ (**13**). This explains the smaller bathochromic shifts caused by the bridge in bis(cyclopentadienyl) complexes than in bis(indenyl) complexes. Part of the observed bathochromic shift could arise from the electron donating ability of the bridge itself, as proposed earlier,[52] but according to an FTIR spectroscopic study of a large group of dicarbonyl complexes $[Cp'_2Zr(CO)_2]$ and electrochemical studies on corresponding metallocene dichlorides, the Me_2Si bridge exerts a net electron withdrawing effect.[72] In the same study it was concluded that the electron withdrawing effect of the interannular bridge is diminished upon increase in its length, the $[CH_2CH_2CH_2]$ bridge being electron donating.

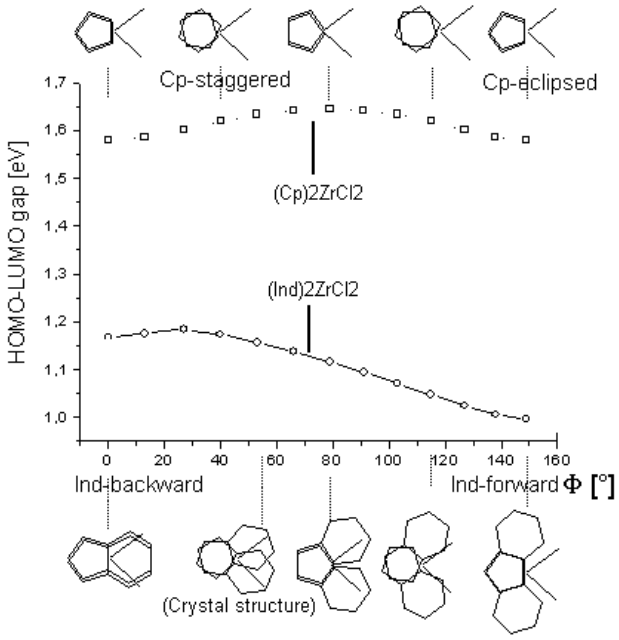

Figure 7. HOMO–LUMO energy differences as a function of the interannular torsion angle ϕ for $(Cp)_2ZrCl_2$ (squares) and $(Ind)_2ZrCl_2$ (circles).[II]

4.4 Bonding angles

Study was made of the effect of the Cp' bonding angles on the LMCT energies of a group of ethylene-bridged siloxy substituted bis(indenyl) zirconocene dichlorides.[I] The position of the siloxy substituent affects the energy of the LMCT transition in both bis(indenyl) complexes **1** and **3** and bis(tetrahydroindenyl) complexes **2** and **4** (Fig. 8). Moving the *t*-Bu(Me)$_2$SiO– group from position 2 to position 1 of the indenyl ring influences the zirconocene geometry. Generally it was observed that increasing the Cp'–Cp' and Cp'–Zr–Cp' angles decreased the LMCT energy. The changes in geometry affect the orbital energies because orientation and overlap of the orbitals have changed. Distortion of the geometry from the optimal bonding angle between the metal and Cp' ligand leads to destabilisation of the HOMO due to reduced overlap of Cp' and Zr orbitals. This, in turn, facilitates the charge transfer and the LMCT occurs at lower energies.[I] The LUMO is less affected by geometry changes because it is nonbonding towards the indenyl ligands. The oxygen of the siloxy group also increases the electron density at the zirconium via direct siloxy–Zr interaction, thus destabilising the LUMO and leading to increased LMCT energy. The siloxy group is closer to the zirconium in the 2-siloxy substituted complex **1** than in its 1-siloxy substituted analogue **3**, the vicinity leading to increased destabilisation of the LUMO.

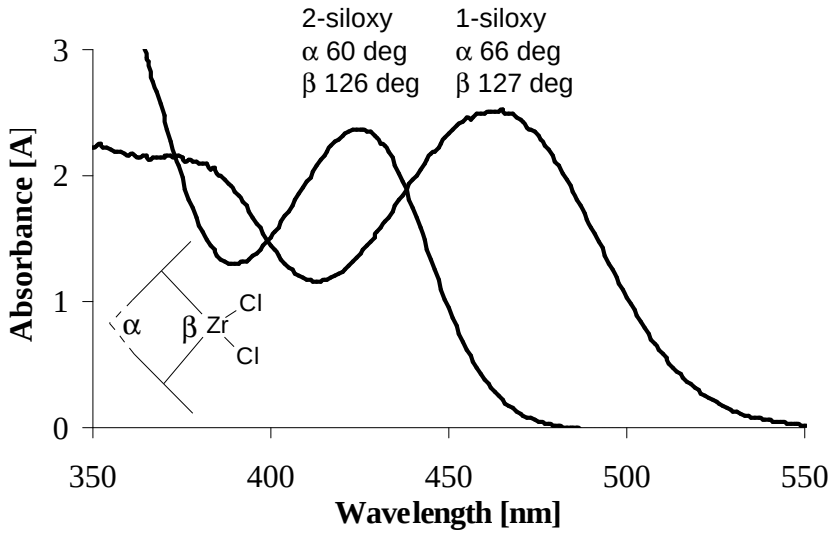

Figure 8. LMCT absorptions and bonding angles of zirconocenes **1** and **3** in toluene.[I]

It needs to be added that bond angles and Ind ligand orientation sometimes change simultaneously. In the case of the siloxy substituted zirconocenes, however, the interannular torsion angles of the complexes were closely similar[73], thus enabling the studies on the effect of bond angles on the LMCT transitions.

5 Effect of a siloxy substituent

Sections 4.1–4.4 discussed the effects of structural changes in group 4 metallocene complexes on the LMCT energy. The LMCT transitions of zirconocene/MAO catalyst systems can be interpreted with reference to these results. A UV/VIS spectroscopic study was made on the effect of a siloxy substituent on the activation behaviour of **6**/MAO based catalyst.

When attached to the ligand framework of a zirconocene catalyst, siloxy groups act as electron donors.[I] The studied siloxy substituted zirconocene dichlorides (**1**–**5**) exhibit higher activities than their unsubstituted analogue (**6**), especially at low [Al]/[Zr] ratios.[43] In the case of the 1-siloxy substituted complex **3** activated with MAO, the catalyst activity in propylene polymerisation decreases and induction times of catalyst activation increase with increasing Al/Zr molar ratio.[45] The activity of the corresponding 1-silyl substituted zirconocene activated with MAO is much lower,[44] which is somewhat surprising since the capability of these two electron donating substituents in stabilising the active cationic species is nearly equal.[38]

The activation behaviour of 1- and 2-siloxy substituted zirconocenes (**3** and **1**, respectively) was compared with the activation of the corresponding 1-silyl (**8**) and unsubstituted (**6**) zirconocenes. UV/VIS spectroscopy revealed that, while the activation of the 2-siloxy, unsubstituted, and 1-silyl substituted complexes proceeds relatively quickly, the activation of the 1-siloxy substituted zirconocene involves three time-consuming reaction steps (Fig. 9).[IV] This is in line with the long induction time observed earlier for the 1-siloxy substituted complex.[44] After the 680 nm band, assigned as a transition state of activation, a band appears at 475 nm (Fig. 9). Probably it arises from a zirconocene species with (siloxy)O–Zr interaction, an

interaction which, according to modelling studies, more easily occurs for the 1-siloxy substituted complex **3** than for its 2-siloxy substituted analogue (**1**).[IV] This shift is followed by the formation of a new band at 525 nm, which presumably arises from the loosening of the (siloxy)O–Zr co-ordination resulting in the stabilisation of LUMO and a decrease in the LMCT energy.

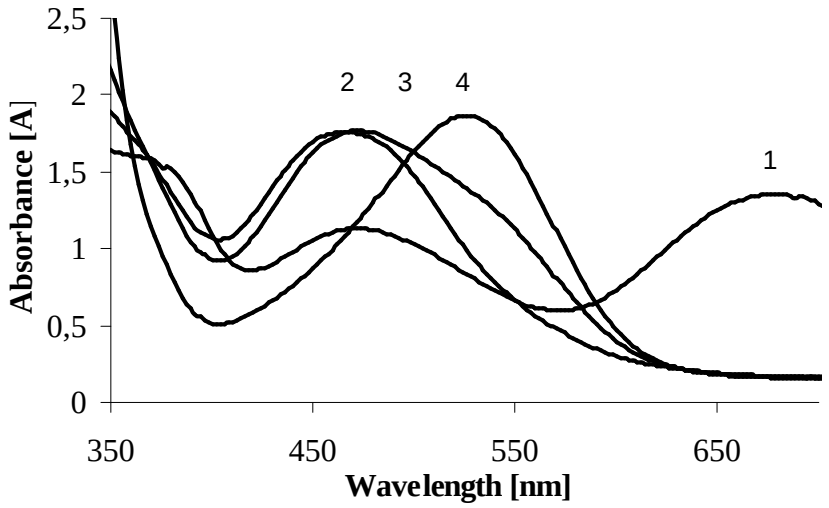

Figure 9. UV/VIS spectra of the 1-siloxy substituted zirconocene (**3**) activated with MAO after 1) 1 min (680 nm), 2) 10 min (475 nm), 3) 1 h (shift from 475 to 525 nm), 4) 7 h (525 nm); [Al]/[Zr]=1700. [IV]

Earlier work of Piccolrovazzi *et al.*[67] has demonstrated that the modest activity of methoxy substituted zirconocenes is due to co-ordination of the Lewis acidic aluminium to the oxygen donor atom of the methoxy group. The resulting inductive electron withdrawal destabilises the active species, leading to a decrease in polymerisation activity relative to the unsubstituted complex. In contrast to this result, siloxy substituted zirconocenes show much higher polymerisation activities than their unsubstituted analogue (**6**).[45] High activities at low activator concentrations are apparently due to the bulkiness of the siloxy group, which hinders the (MAO)Al–O(siloxy) interaction.[38]

^{29}Si NMR spectroscopy was used to study the (TMA)Al–O(siloxy) interaction as a model for the (MAO)Al–O(siloxy) interaction. The (TMA)Al–O(siloxy) interaction

was not observed at [Al]/[Zr]=40, *i.e.* the silicon peak in the spectrum was not shifted in the presence of TMA.[IV]

Although Al–O(siloxy) interaction was not observed at [Al]/[Zr] ratio of 40, the interaction became significant at higher [Al]/[Zr] ratios. Polymerisation results have indeed shown that the activity of the **3**/MAO catalyst system decreases with increasing [Al]/[Zr] ratio.[43] In the UV/VIS spectrum of **3**/MAO (Fig. 10) an LMCT band shift back to higher energies was detected at [Al]/[Zr]>7500. This result indicates changes in the active sites, caused by (MAO)Al–O(siloxy) interaction, for example.[IV]

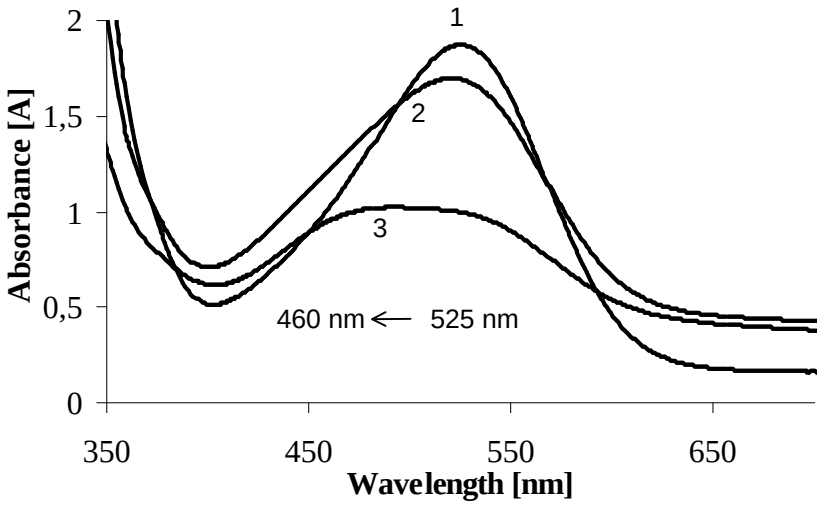

Figure 10. UV/VIS spectra of 1-siloxy substituted zirconocene **3** with MAO after 6 hours reaction time: [Al]/[Zr] is 1) 1700, 2) 7500 and 3) 15 000.[IV]

Molecular modelling studies on the interaction between the Lewis acidic aluminium of TMA and the oxygen atoms of methoxy (**7**) and siloxy (**1** and **3**) substituted catalyst precursors were performed for further investigation of the Al–O(siloxy) interaction. For the methoxy substituted complex (**7**), which has low activity, the Al–O(methoxy) interaction was found to be spontaneous, whereas the bulky siloxy substituents were capable of blocking TMA and making the Al–O(siloxy) interaction unfavourable. The blocking was calculated to be more pronounced with the 2-siloxy substituent (complex **1**) than the 1-siloxy substituent (complex **3**). The role of the siloxy substituent in the activation behaviour of the zirconocene was concluded to be

the following: a) in the 1-siloxy substituted complex **3** the (siloxy)O–Zr interaction slows down the activation process, whereas in the 2-siloxy substituted complex **1** the interaction is too weak to affect the activation process; b) the (MAO)Al–O(siloxy) interaction is hindered by the bulkiness of the siloxy group; and c) although the (MAO)Al–O(siloxy) interaction is not feasible at low [Al]/[Zr] ratios, at very high [Al]/[Zr] ratios it becomes significant for the 1-siloxy substituted complex **3**.

6 Predicting catalyst activity from LMCT

For research purposes, group 4 metallocene catalyst activity is usually determined by laboratory-scale polymerisation, which is both time and resource consuming. As demonstrated in section 5, UV/VIS spectroscopy provides a useful tool for optimising the catalyst, for example [Al]/[Zr] ratios and pre-contact times, before full polymerisation studies. A direct interdependency has been found between the LMCT absorption and catalyst activity: decrease in LMCT absorption energy with increasing MAO concentration was demonstrated to correlate with increasing activity in olefin polymerisation.[24,74] The correlation was suggested to arise from the increased positive charge of the zirconocene cation due to ion pair dissociation at high MAO concentrations. Conductivity experiments supported this proposal—higher conductivities were recorded at higher [Al]/[Zr] ratios.[24]

This relationship between catalyst activity and LMCT absorption energy is valid only when different forms of the same catalyst are compared, *e.g.* $Et(Ind)_2ZrCl_2$ with variable amounts of MAO. The comparison of different complexes is less straightforward because their structures have an effect on the LMCT energy, as discussed above. A correlation between activity and LMCT of different complexes can be seen if the complexes are of relatively similar structure, *i.e.* there are no notable differences in the substitution pattern or the bridge structure. This was the case for the siloxy substituted zirconocenes **1–5**: the correlation between activity and LMCT absorption energy was found for dichloride, methylated and cationic forms of the complexes.[III] Complex **6** clearly does not belong to the siloxy substituted complex

group and does not follow the discovered trend of increasing catalyst activity with increasing LMCT energy (Fig. 11).

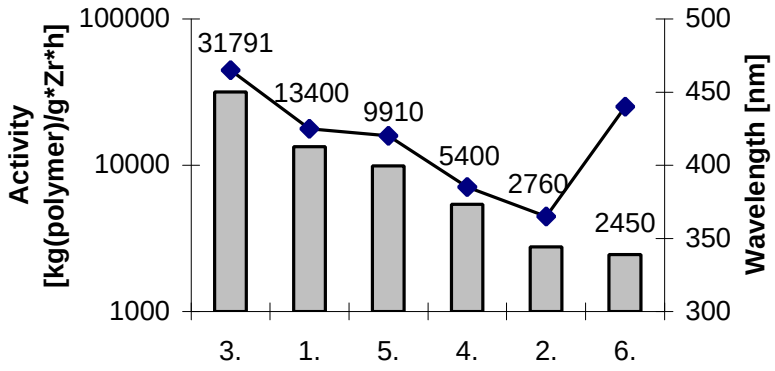

Figure 11. Correlation between the ethylene/hexene co-polymerisation activity (activation with MAO, [Al]/[Zr]=1000) and the lowest energy LMCT absorption (♦) of complexes **1**–**6** in the dichloride form.[III]

The trend seen in Fig. 11 could be interpreted to originate from the different state of the electron deficiency at the zirconium centre of the activated complexes. Frontier orbital investigations revealed an alternative explanation: the LMCT absorption energy is reduced by stabilisation of the LUMO, which is mainly of metal character, and by destabilisation of the Cp' ligand based HOMO.[III] Charge transfer to the metal is facilitated with increasing stability of the LUMO. Thus, also the replacement of electron withdrawing chlorides with electron donating methyl groups becomes more favourable. Destabilisation of the HOMO favours cation formation by methyl or chlorine abstraction. This is due to facilitation of the charge transfer from ligand to metal, which stabilises the active cationic species. The LMCT absorption energy thus indicates the facility of a metallocene dichloride to undergo methylation and cationisation.[III]

The cationisation of monomethyl zirconocene includes a chloride abstraction step to give the cationic complex. As discussed above, cation formation should be favoured by the destabilised HOMO. Since the HOMO has been calculated to be more stable in monomethyl zirconocenes than in their dimethyl analogues[III], the cationisation of a dimethyl complex can be expected to be more favourable. To demonstrate this effect,

the activation behaviour of **1** was compared with the activation behaviour of **1**–Me_2. Both catalysts reached the final cationic form in less than 5 minutes, suggesting similar activation kinetics. As expected, the reaction of the complexes with MAO ([Al]/[Zr]=1000) resulted in LMCT bands with exactly the same energy, indicating the same cationic species. Although the LMCT energies of the complexes were the same, the activated complex **1** nevertheless absorbed at lower intensity than the activated complex **1**–Me_2, which according to Beer's law indicates lower concentration of active species. This was supported by the polymerisation results—the activity of complex **1** was lower than the activity of complex **1**–Me_2 (Fig. 12).[III]

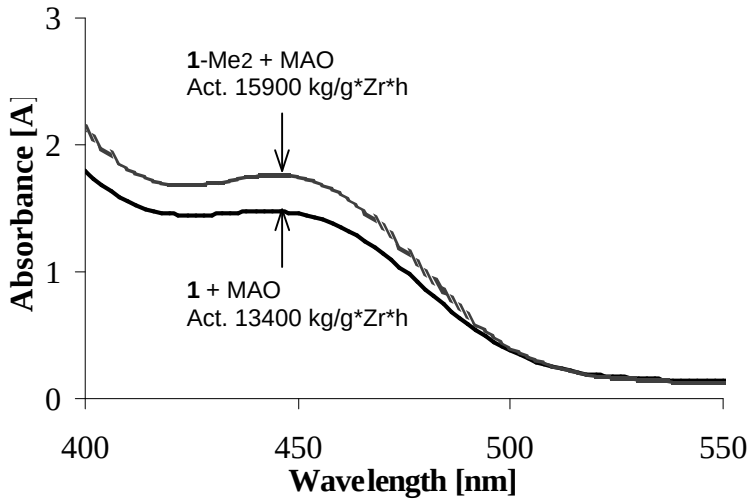

Figure 12. LMCT transitions and polymerisation activities of complex **1** and complex **1**–Me_2 activated with MAO ([Al]/[Zr]=1000, contact time 2 h).[III]

With the correlation between the LMCT energy and the activity now established, a metallocene complex with an optimal, narrow HOMO–LUMO energy gap, producing a catalyst with maximal activity, can be designed on the basis of the information from section 4 (Fig. 13). A decrease in the HOMO–LUMO gap requires that the HOMO is destabilised and the LUMO stabilised. As described in section 4, the factors destabilising the HOMO are: a) electron donating substituents in the Cp' ligand[I, II], b) large Cp'–Cp' and Cp'–M–Cp' bond angles[I], c) a large Cp'–Cp' torsion angle[II] and d) the use of methylated metallocenes instead of metallocene dichlorides[III]. Factors stabilising the LUMO were concluded to be: a) the lack of co-ordination of the electron donating substituent to the metal[IV] and b) the replacement of hafnium with

zirconium. It must be borne in mind that these general conclusions are based on electonic factors and do not take the steric factors into account. For example, while short bridges result in favoured large Cp'–Cp' bond angles they usually have an unfavourable influence on shielding and stability of the active metallocene cation.

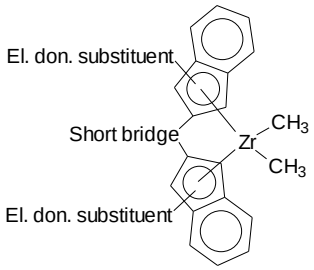

Figure 13. An indicative sketch of a zirconocene with an optimal narrow HOMO–LUMO energy gap resulting in high activity in ethylene polymerisation.

Sections 5 and 6 have demonstrated that UV/VIS spectroscopy can usefully be applied in studies on catalyst activation. In the case of uniform metallocene groups, a correlation can be established between LMCT energy and catalyst activity. In the following section the application of UV/VIS spectroscopy is extended to the identification of catalyst species attached on a support material.

7 Effect of catalyst supporting

Current polymerisation technologies are mostly based on gas phase or slurry processes in which the catalyst should be able to produce polymer particles with desired morphology. The metallocene catalyst is thus often attached on a support material, the choice of which is dictated by specific requirements. The support material should be of low reactivity with respect to catalyst deactivation but at the same time sufficiently reactive with the catalyst to prevent its leaching from the support. The most commonly used support material is partially dehydroxylated porous silica.

The support has both negative and positive effects on the catalyst behaviour. In general, the activity of supported metallocene catalysts is lower than that of the corresponding homogeneous systems in olefin polymerisation because the diffusion of monomer into the pores of the catalyst is slower and the number of active centres is reduced.[75,76] In the case of zirconocene systems, an important advantage of supported catalysts is their lower requirement for the activator (MAO): a large excess of MAO ([Al]/[Zr]>1000) is necessary for the unsupported catalyst, whereas considerably smaller amounts ([Al]/[Zr]=50–300) suffice for supported systems with similar activities.[31,77] The reduction of bimolecular deactivation in the supported systems relative to the homogeneous catalysts has been suggested as the reason for this difference.[78]

7.1 Earlier characterisation studies

Despite the industrial interest in supported metallocene catalysts, only a few studies have been published on the species formed in reactions between the support, the metallocene and MAO. Focus has more often been on the reactions and interactions between silica and metallocene[79] than on the complete catalyst system. Rutherford backscattering (RBS) and FTIR spectroscopic studies have shown that when (*n*-$BuCp)_2ZrCl_2$ reacts with partially dehydroxylated silica the concentration of hydroxyl groups on the silica support steers the reaction of zirconocene in either a mono- or a bidentate way.[80] Monodentate species are active in olefin polymerisation, whereas bidentate species are inactive. In the studies in question[80] MAO was added to the polymerisation reactor and not to the catalyst. In a related study,[81] XPS indicated the presence of two types of ion pairs, one assumed to be $[SiO]^-[Et(Ind)_2ZrCl]^+$ and the other a trapped multi co-ordinated crown complex of $[Et(Ind)_2ZrCl]^+$ and MAO^-. The ratio of the two species was found to depend on the method used to prepare the heterogeneous system, and omitting MAO led to $[SiO]^-[Et(Ind)_2ZrCl]^+$ being the sole product. When $Et(Ind)_2ZrCl_2$ was immobilised on the surface of mesoporous silica and then modified with MAO, the EXAFS of the resulting system revealed that the bonds between the metal and chloride groups were broken,[82] whereas the bonds within the indenyl ligand framework remained intact. As expected, a Zr–C bond consistent with the $Zr^+–CH_3$ fragment was also observed.

In a study of the catalyst system SiO_2/MAO/Et(Ind)$_2ZrCl_2$ by UV/VIS, diffuse reflectance FTIR and XPS spectroscopies, Soga *et al.* [83] concluded that the catalyst consists of methylated, not cationic, zirconocene species, which is reasonable since they used very low [Al]/[Zr] ratios of 4–66. These catalysts required further MAO addition to the polymerisation reactor.

There are differences in behaviour between catalysts pretreated with MAO and nonpretreated ones. When a metallocene is supported on partially dehydroxylated MAO-treated silica, stereochemical analysis of the polypropylene product shows a product profile very similar to the one obtained with the corresponding homogeneous catalyst. This is consistent with the hypothesis that the active sites in the homogeneous and heterogeneous systems are similar. [76,84] However, catalytic activity is significantly reduced when the metallocene is first supported and then activated with MAO in the polymerisation reactor. The product also exhibits a considerably different microstructure to the polymer produced using corresponding homogeneous catalyst.[83] On the basis of these studies, the method of preparation of supported catalysts and the pre-treatment of the silica can be concluded to affect the nature of the catalytically active species. This conclusion is of industrial and economic significance because the active species dictates the behaviour of the catalyst in the olefin polymerisation process.

7.2 Characterisation of supported hafnocene catalysts

This section reports the characterisation of the relatively little studied hafnocene based catalyst systems.[V,85] The species on supported olefin polymerisation catalysts consisting of complex (*n*-BuCp)$_2HfCl_2$ (**16**), MAO and partially dehydroxylated porous silica were identified by EXAFS and UV/VIS spectroscopy. According to EXAFS the reaction of **16** with silica leads to a product containing Hf–O and Hf–Si nonbonded interactions and approximately 50% of the hafnocene has lost a chlorine ligand. The results indicate the formation of cationic hafnocene monochloride species, as observed earlier by XPS.[81] These $[SiO]^-[(n\text{-BuCp})_2Hf(Cl)]^+$ species presumably give rise to one of the absorption bands (450 nm or 570 nm) in the UV/VIS spectra seen in Fig. 14. The other UV/VIS absorption band is assumed to originate from

nonbonded interactions between **16** and the silica oxygens. It is worth noting that the absorptions of the possible residues of pure hafnocene (300 nm and 315 nm) are very weak indicating efficient interaction of hafnocene with silica.

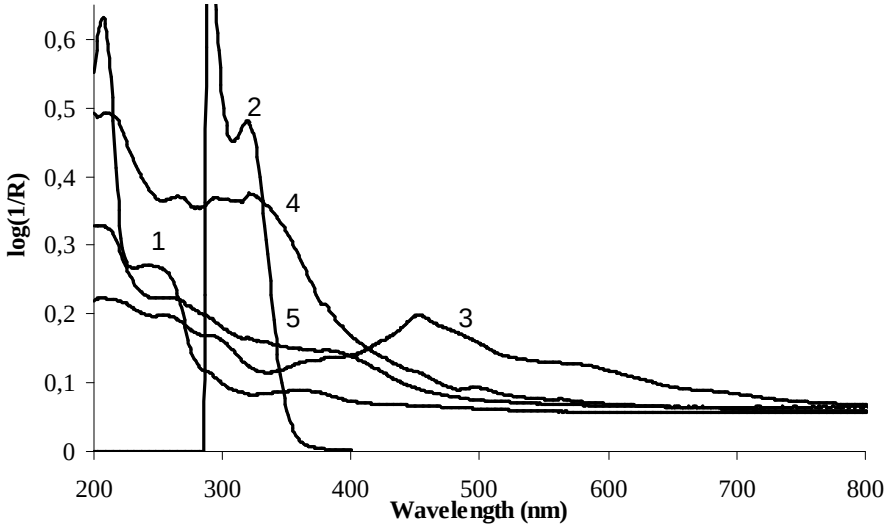

Figure 14. UV/VIS spectra of 1) SiO_2, 2) complex **16**, 3) SiO_2/**16**, 4) SiO_2/MAO/**16** and 5) SiO_2/(MAO+**16**). Spectra were collected in reflectance mode, except the spectrum of complex **16**, which was collected in absorbance mode with the complex dissolved in toluene.[V]

When MAO is included in the SiO_2/**16** sample (curves 4 and 5 in Fig. 14), the absorptions at 450 and 570 nm in the UV/VIS spectrum disappear. Evidently direct hafnocene–silica interactions are then reduced in number and instead a new absorption band at about 380 nm begins to form. With the same methodology applied for interpretation of UV/VIS spectra as for the homogeneous catalyst in sections above, this band can be concluded to indicate a cationic hafnocene complex because the cationic hafnocene, $(n\text{-BuCp})_2Hf(CH_3)^+$, should have its Cp'→Hf LMCT absorption at lower energies than the hafnocene dichloride, **16**. EXAFS revealed the presence of several types of hafnium environments in the silica/MAO/**16** catalyst, which is consistent with the presence of different hafnocene species.

The UV/VIS absorption spectrum shows a significant fraction of unreacted hafnocene present in the catalyst SiO_2/MAO/**16** (curve 4, Fig. 14). In the sample SiO_2/**16** (curve 3, Fig. 14), only a negligible portion of unreacted **16** was observed. This indicates that

the reaction of hafnocene was less efficient with MAO-treated than with pure silica. In SiO_2/(MAO+**16**) the complex **16** was allowed to react with MAO before being supported on silica, which explains the low absorption intensity of the unreacted hafnocene.

8 Effect of light irradiation

Metallocene catalysts contain a mixture of active and inactive species in dynamic equilibrium with each other. The two major catalyst components, metallocene and MAO, are both rather costly, and shifts in the equilibrium towards the active species are desired by the polyolefin industry. The means to adjust the equilibrium vary with the catalyst system—the activity of some metallocene/MAO combinations can be enhanced by increasing the temperature, for example, while some other catalysts are deactivated at elevated temperatures.[86]

In polymerisation studies, Kallio *et al.*[87] observed irradiation of the polymerisation system with halogen light to increase the ethylene polymerisation activity of (*n*-BuCp)$_2$$ZrCl_2$/MAO/$SiO_2$ (**17**/MAO/SiO_2) catalyst. They also found that the activation effect of light is more pronounced when the polymerisation system is contaminated by oxygen. Through introduction of light to the contaminated polymerisation system, catalyst activity was recovered.[88] The reasons for this phenomenon were studied here by UV/VIS spectroscopy.[VI]

Vinylcyclohexane (VCH) was used to study the reactivity of the zirconocene catalyst towards monomer. As can be seen in Fig. 15, the spectral shifts were more pronounced when the **17**/MAO/VCH system was irradiated with visible light between the UV/VIS measurements, indicating higher reactivity of VCH with the catalyst in the presence of light (Fig. 15).

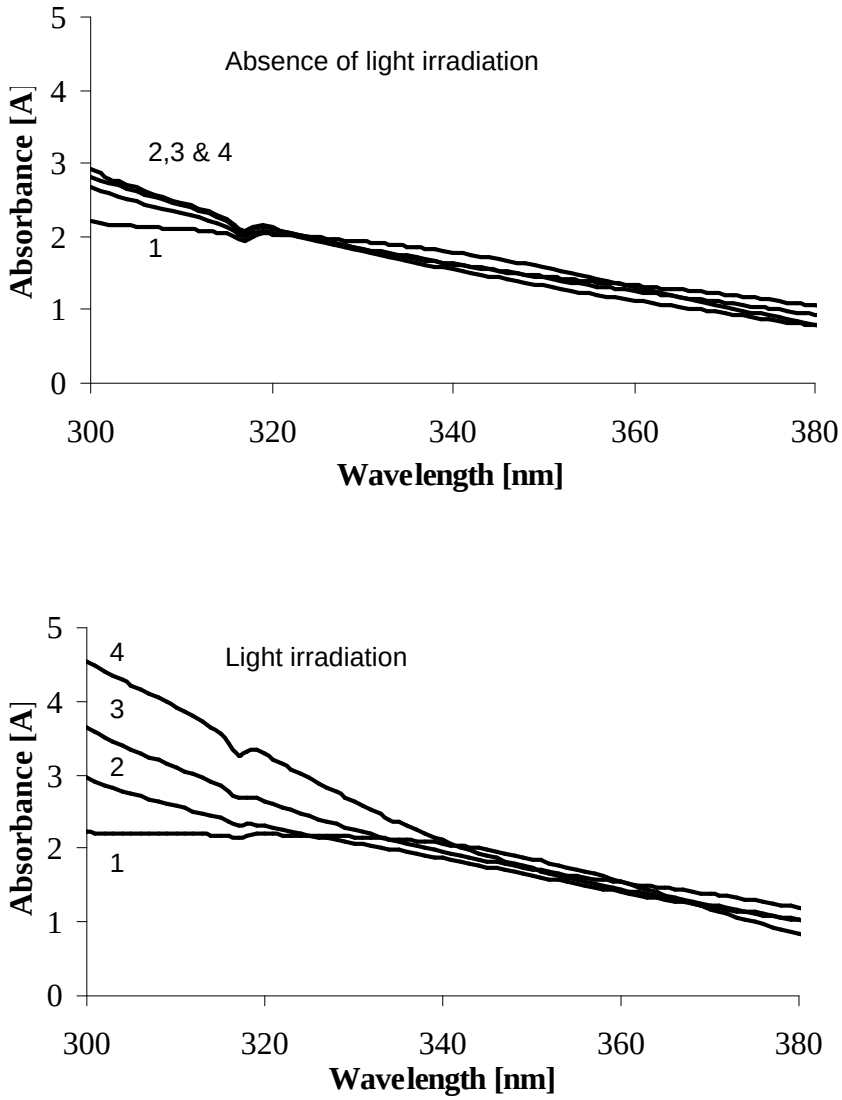

Figure 15. Absorption spectra of **17**/MAO 1) without VCH and with VCH after 2) 5 min, 3) 1 h and 4) 5 h. Measurements were done at room temperature and ratios [Al]/[Zr]=200, [VCH]/[Zr]=100 were used. In the upper figure the samples were kept in dark between the measurements, while in the figure below they were irradiated continuously between the measurements.[VI]

UV/VIS spectroscopic studies revealed that **17**/MAO is not very sensitive towards oxygen, *i.e.* only at $[O_2]/[Zr]$ ratios higher than 100 were changes seen in the UV/VIS spectrum of the active catalyst. For the **17**/MAO/VCH system, even low concentrations of oxygen, $[O_2]/[Zr]=1–10$, were sufficient to decrease the 300 nm absorption intensity, indicating reduced VCH interaction with the catalyst (Fig. 16). This result suggests that O_2 interaction with the cationic zirconium centre occurs in

such a way that monomer reactions become hindered. Similarly to the reported recovery of polymerisation activity,[88] light irradiation recovered the 300 nm species to their corresponding nonpoisoned level (Fig. 16). The role of irradiation was accordingly concluded to be detaching the poisoning species, *e.g.* O_2, from the active centre to allow the monomer to react more effectively.

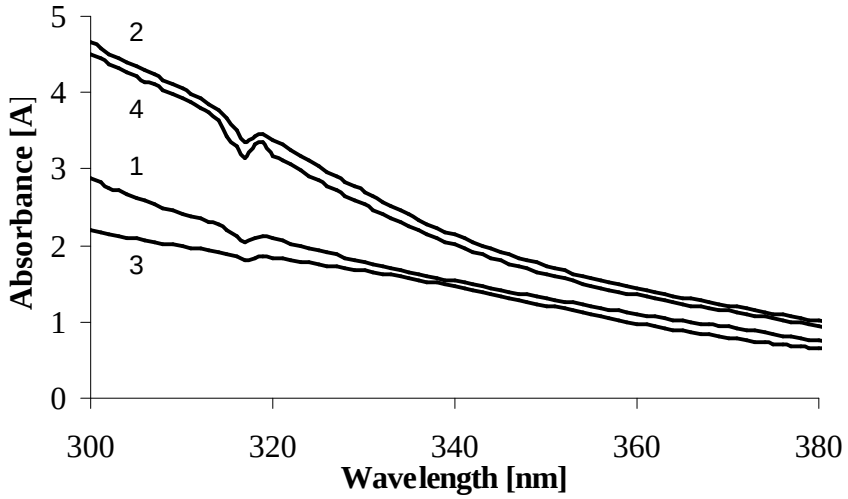

Figure 16. Absorption spectra of catalyst system **17**/MAO/VCH measured 1) in dark, 2) irradiated, 3) with added O_2 in dark, 4) with added O_2, irradiated. Conditions: six hours reaction, [VCH]/[Zr]=100, [Al]/[Zr]=200 and [O_2]/[Zr]=1 with measurements performed in toluene at room temperature.[VI]

According to ^{1}H NMR, the structure of the reaction product formed in the **17**/MAO/VCH system by irradiation closely resembles the structure of the VCH product obtained without irradiation. This suggests that the reaction itself does not change with irradiation. Further support for this suggestion is provided by the structural characterisation of polyethylene produced in light and in dark.[89]

Conclusions

The effect of changes in the metal centre, Cp' ligand substitution, Cp'–Cp' and Cp'–Zr–Cp' bond angles and interannular torsion angle on the LMCT transitions of group 4 metallocene complexes was studied by UV/VIS spectroscopy. The LMCT energy decreases in the order hafnocene > zirconocene > titanocene and as the electron donating ability of the substituent increases. An increase in bond angles leads to a decrease in the LMCT absorption energy. In general, distortion of the geometry from the optimal overlap angle between the metal based LUMO and Cp' ligand based HOMO orbitals leads to destabilisation of the HOMO and stabilisation of the LUMO, which results in a decreased HOMO–LUMO energy gap and LMCT energy.

A correlation between the LMCT energy and catalyst polymerisation activity was established within a uniform group of complexes. Decreasing LMCT energy was observed to correlate with increasing activity. Since LMCT is a measure of the HOMO–LUMO energy gap, increase in catalyst activity is favoured by factors destabilising the HOMO and stabilising the LUMO.

The catalyst activation behaviour of a group of zirconocene complexes was followed by UV/VIS spectroscopy. In the case of the 1-siloxy substituted zirconocene (**3**) the Zr–O(siloxy) interaction was concluded to cause the long induction period observed in olefin polymerisation. (MAO)Al–O(siloxy) interaction was not found at low [Al]/[Zr] ratios, but the interaction was observed at [Al]/[Zr]>7500. This is in line with decreasing polymerisation activity at increasing [Al]/[Zr] ratios.

EXAFS and UV/VIS spectroscopy were used to study (*n*-BuCp)$_2$HfCl$_2$/MAO/silica based catalysts. (*n*-BuCp)$_2$HfCl$_2$ interacts with silica by losing one chlorine ligand and via Hf–O and Hf–Si nonbonded interactions. It reacts with MAO-treated silica less efficiently than with pure silica and produces a mixture of unreacted hafnocene, hafnocene–silica species and different cationic hafnocene species.

Light irradiation of the polymerisation system has been observed to increase the catalyst activity significantly. UV/VIS spectroscopy showed that the irradiation does

not result in changes in the catalyst or the catalyst/monomer reaction products, but it enhances catalyst reactivity with the olefin monomer. When oxygen is added to the catalyst system it interacts with the active zirconium centres decreasing the catalyst activity. Light irradiation of this oxygen-poisoned system recovers the catalyst activity by favouring the reactivity of the zirconium with the monomer rather than oxygen. It was also observed that the catalyst with added monomer is much more reactive towards oxygen than the catalyst without added monomer.

This work demonstrates that UV/VIS spectroscopy can be used as a powerful tool in metallocene catalyst research. It gives valuable information on: (a) the electronic structure of metallocenes, (b) the reactions of metallocenes with activator, monomer, catalyst poisons and other components under various conditions, (c) reaction kinetics and (d) catalyst supporting.

References

1. Montagna, A. A.; Burkhart, R. M.; Dekmezian, A. H. *CHEMTECH* **1997**, *27(12)*, 26.

2. Kealy, T. J.; Pauson, P. L. *Nature (London)* **1951**, *168*, 1039.

3. Miller, S. A.; Tebboth, J. A.; Tremaine, J. F. *J. Chem. Soc.* **1952**, 632.

4. Wilkinson, G.; Rosenblum, M.; Whiting, M. C.; Woodward, R. B. *J. Am. Chem. Soc.* **1952**, *74*, 2125.

5. Wilkinson, G. *J. Organomet. Chem.* **1975**, *100*, 273.

6. Natta, G.; Pino, P.; Mazzanti, G.; Giannini, U. *J. Am. Chem. Soc.* **1957**, *79*, 2975.

7. Breslow, D. S.; Newburg, N. R. *J. Am. Chem. Soc.* **1957**, *79*, 5072.

8. (a) Reichert, K. H.; Meyer, K. R. *Macromol. Chem.* **1973**, *169*, 163. (b) Long, W. P.; Breslow, D. S.; *Liebigs Ann. Chem.* **1975,** 463.

9. (a) Andersen, A.; Cordes, H. G.; Herwig, H.; Kaminsky, W.; Merck, A.; Mottweiler, R.; Peir, J.; Sinn, H.; Vollmer, H. J., *Angew. Chem., Int. Ed. Engl.* **1976**, *15*, 630. (b) Sinn, H.; Kaminsky, W.; Vollmer, H. J.; Woldt, R., *Angew. Chem., Int. Ed. Engl.* **1980**, *19*, 390.

10. Wild, F. R. W. P.; Wasiucionek, M.; Huttner, G.; Brintzinger, H-H., *J. Organomet. Chem.* **1985**, *288*, 63.

11. (a) Kaminsky, W.; Külper, K.; Brintzinger, H. H.; Wild, F. R.; *Angew. Chem.* **1985**, *97*, 507. (b) Kaminsky, W.; Arndt, M. *Adv. Polym. Sci.* **1997**, *127*, 143.

12. Garbassi, F.; Gila, L.; Proto, A. *Polymer News* **1994**, *19*, 367.

13. See, for example, the following reviews and references therein: (a) Brintzinger, H. H.; Fischer, D.; Mülhaupt, R.; Rieger, B.; Waymouth, R. M. *Angew. Chem., Int. Ed. Engl.* **1995**, *34*, 1143. (b) Kaminsky, W. *Macromol. Chem. Phys.* **1996**, *197*, 3907. (c) Hlatky, G. G. *Chem. Rev.* **2000**, *100*, 1347.

14. Metallocene catalysts are used, for example, to produce polyethylene for rotomoulding applications. www.borecene.com

15. Long, N. J. *Metallocenes*, Blackwell Science Ltd., **1998**.

16. Piemontesi, F.; Camurati, I.; Resconi, L.; Balboni, D.; Sironi, A., Moret, M.; Zeigler, R.; Piccolrovazzi, N. *Organometallics* **1995**, *14*, 1256.

17. Togni, A.; Halterman, R. L.: Eds. *Metallocenes: Synthesis, Reactivity, Applications*, Wiley–VCH, Weinheim, **1998**.

18. (a) Harlan, C. J.; Mason, M. R.; Barron, A. R. *Organometallics* **1994**, *13*, 2957. (b) Chen, E. Y.; Marks, T. J. *Chem. Rev.* **2000**, *100*, 1391. (c) Ystenes, M.; Eilertsen, J. L.; Liu, J.; Ott, M.; Rytter, E.; Stovneng, J. A. *J. Polym. Sci., Part A: Polym. Chem.* **2000**, *38*, 3106. (d) Zurek, E.; Woo, T. K.; Firman, T.; Ziegler, T. *Inorg. Chem.* **2001**, *40*, 361. (e) Zakharov, V. A.; Talzi, E. P.; Babushkin, D. E.; Semikolenova, N. V. *Kin. and Catal.* **1999**, *40*, 836.

19. Gassmann, P. G.; Callstrom, M. R. *J. Am. Chem. Soc.* **1987**, *109*, 7875.

20. (a) Eisch, J. J.; Pombrick, S. I.; Zheng, G. X. *Organometallics* **1993**, *12*, 3856. (b) Sishta, C.; Halthorn, R. M.; Marks, T. J. *J. Am. Chem. Soc.* **1992**, *114*, 1112.

21. (a) Siedle, A. R.; Newmark, R. A.; Gleason, W. B.; Lamanna, W. M. *Organometallics* **1990**, *9*, 1290. (b) Bühl, M.; Hopp, G.; von Philipsborn, W.;

Beck, S.; Prosenc, M. H.; Rief, U.; Brintzinger, H. H. *Organometallics* **1996**, *15*, 778.

22. Bochmann, M. *J. Chem. Soc., Dalton Trans.*, **1996**, 255.

23. van Beek, J. A. M.; Pieters, P. J. J.; van Tol, M. F. H. Proceedings of symposium *Metallocenes '95*, Brussels, April 26–27 (**1995**).

24. (a) Coevoet, D.; Cramail, H.; Deffieux, A. *Macromol. Chem. Phys.* **1998**, *199*, 1451. (b) Coevoet, D.; Cramail, H.; Deffieux, A. *Macromol. Chem. Phys.* **1998**, *199*, 1459.

25. Tritto, I., Li, S.; Sacchi, M. C.; Zannoni, G. *Macromolecules* **1993**, *26*, 7112.

26. Cam, D.; Giannini, U. *Macromol. Chem.* **1992**, *193*, 1049.

27. (a) Tritto, I.; Li, S.; Sacchi, M. C.; Locatelli, P.; Zannoni, G. *Macromolecules* **1995**, *28*, 558. (b) Tritto, I.; Sacchi, M. C.; Li, S. X. *Macromol. Symp.* **1995**, *89*, 289. (c) Tritto, I.; Sacchi, M. C.; Li, S. X. *Macromol. Symp.* **1995**, *97*, 101.

28. Tritto, I.; Donetti, R.; Sacchi, M. C.; Locatelli, P.; Zannoni, G. *Macromolecules* **1997**, *30*,1247.

29. Bochmann, M.; Lancaster, S. J. *Angew. Chem. Int. Ed. Engl.* **1994**, *33*, 1634.

30. Möhring, P.; Coville, N. *J. Organomet. Chem.* **1994**, *479*, 1.

31. Kaminsky, W. *Macromol. Symp.* **1995**, *97*, 79.

32. Bochmann, M.; Cuenca, T.; Hardy, D. T, *J. Organomet. Chem.* **1994**, *484*, 10.

33. (a) Cossee, P. *J. Catal.* **1964**, *3*, 80. (b) Arlman, E. J., Cossee, P. *J. Catal.* **1964**, *3*, 99.

34. (a) Ivin, K. J.; Rooney, J. J.; Stewart, C. D.; Green, M. L. H.; Mahtab, R., *J. Chem. Soc. Chem. Commun.* **1978**, 604. (b) Green, M. L. H., *Pure Appl. Chem.* **1978**, *50*, 27. (c) Lavery, D. T.; Rooney, J. J. *J. Chem. Soc. Faraday Trans.* **1983**, *79*, 869.

35. Brookhart, M.; Green, M. L. H., *J. Organomet. Chem.* **1983,** *250*, 395.

36. (a) Grubbs, R. H.; Coates, G. W. *Acc. Chem. Res.* **1996**, *29*, 86. (b) Krauledat, H.; Brintzinger, H. H. *Angew. Chem. Int. Ed. Engl.* **1990**, *29*, 1412. (c) Piers, W. E.; Bercaw, J. E. *J. Am. Chem. Soc.* **1990**, *112*, 9406.

37. Crabtree, R. H. *The organometallic chemistry of the transition metals*, Wiley Inter-science, New York, 2nd ed. **1994** pp. 294–298.

38. Linnolahti, M.; Pakkanen, T. A. *Macromolecules* **2000**, *33*, 9205.

39. Repo, T. *Doctoral Dissertation*: *Studies of Steric Interactions in Metallocene Catalyzed Olefin Polymerisation*, University of Helsinki, **1997**.

40. (a) Schnutenhaus, H.; Brintzinger, H. H.; *Angew. Chem.* **1979**, *91*, 837. (b) Smith, J. A.; von Seyerl, J.; Huttner, G.; Brintzinger, H. H. *J. Organomet. Chem.* **1979**, *173*, 175. (c) Smith, J. A.; Brintzinger, H. H. *J. Organomet. Chem.* **1981**, *218*, 159.

41. (a) Leino, R. *Doctoral Dissertation: Siloxy Substituted Metallocene Catalysts*, Åbo Akademi University, **1998**. (b) Luttikhedde, H. J. G. *Doctoral Dissertation: Structural Variations in Group IV bis(indenyl) Metallocenes*, Åbo Akademi University, **1998**.

42. (a) Leino, R.; Luttikhedde, H.; Wilén, C-E.; Sillanpää, R.; Näsman, J. H. *Organometallics* **1996**, *15*, 2450. (b) Luttikhedde, H. J. G.; Leino, R.; Lehtonen, A.; Näsman, J. H. *J. Organomet. Chem.* **1998**, *555*, 127. (c) Leino, R.; Luttikhedde, H. J. G.; Lehtonen, A.; Ekholm, P.; Näsman, J. H. *J. Organomet. Chem.* **1998**, *558*, 181.

43. Leino, R.; Luttikhedde, H. J. G.; Lehmus, P.; Wilén, C. Sjöholm, R.; Lehtonen, A.; Seppälä, J. V.; Näsman, J. H. *Macromolecules,* **1997**, *30*, 3477.

44. Lehmus, P.; Kokko, E.; Härkki, O.; Leino, R.; Luttikhedde, H.; Näsman, J. H.; Seppälä, J. *Macromolecules,* **1999**, *32*, 3547.

45. Ekholm, P.; Lehmus, P.; Kokko, E.; Haukka, M.; Seppälä, J.; Wilen, C-E. *J. Polym. Sci. A: Polym. Chem.* **2001**, *39*, 127.

46. Gassman, P. G.; Macomber, D. W.; Hershberger, J. W. *Organometallics* **1983**, *2*, 1470.

47. Gassman, P. G.; Macomber, D. E.; Willging, S. M. *J. Am. Chem. Soc.* **1985**, *107*, 385.

48. Garbassi, F.; Gila, L.; Proto, A. *J. Mol. Catal. A: Chem.* **1995**, *101*, 199.

49. Gassman, P. G.; Winter, C. H. *Organometallics* **1991**, *10*, 1592.

50. Möhring, P. C.; Coville, N. J. *J. Mol. Catal. A: Chem* **1992**, *77*, 41.

51. (a) Beck, S.; Brintzinger, H. H. *Inorg. Chim. Acta* **1998**, *270*, 376. (b) exchange rection also studied in Siedle, A. R.; Newmark, R. A.; Lamanna, W. M.; Schoepfer, J. N. *Polyhedron* **1990**, *9*, 301. (c) Ott, K. C.; deBoer, E. J. M.; Grubbs, R. H. *Organometallics* **1984**, *3*, 223.

52. Wieser, U.; Babushkin, D.; Brintzinger, H. H. *Organometallics*, **2002**, *21*, 920.

53. Herfert, N.; Fink G. *Macromol. Chem. Rap. Commun.* **1993**, *14*, 91.

54. Babushkin, D. E.; Semikolenova, N. V.; Zakharov, V. A.; Talsi, E. P. *Macromol. Chem. Phys.* **2000**, *201*, 558.

55. Zurek, E.; Ziegler, T. *Organometallics* **2002**, *21*, 83.

56. (a) Denney, R. *Visible and Ultraviolet Spectroscopy*, John Wiley & Sons, **1987**. (b) Rao, C. N- R. *Ultra-Violet and Visible Spectroscopy, Chemical Applications*, Butterworths, **1961**, London. (c) Jaffé, H. H.; Orchin, M. *Theory and Applications of Ultravolet Spectroscopy*, John Wiley and Sons, Inc., **1962**.

57. (a) Pédeutour, J.; Coevoet, D.; Cramail, H.; Deffieux, A. *Macromol. Chem. Phys.* **1999**, *200*, 1215. (b) Ferreira, M. L.; Belelli, P. G.; Damiani, D. E. *Macromol. Chem. Phys*. **2001**, *202*, 495. (c) Pédeutour, J.; Coevoet, D.; Cramail, H.; Deffieux, A. *J. Mol. Catal. A: Chem.* **2001**, *176*, 87.

58. Unpublished results by the author.

59. Pédeutour, J.; Radhakrishnan, K.; Cramail, H.; Deffieux, A. *J. Mol. Catal. A: Chem.* **2002**, *185*, 119.

60. Pédeutour, J.; Coevoet, D.; Cramail, H.; Deffieux, A. *J. Mol. Catal. A. Chem.* **2001**, *174*, 81.

61. Wieser, U.; Brintzinger, H. H. *Organometallic Catalysts and Olefin Polymerization*, Ed.: Blom, R.; Follestad, A.; Rytter, E.; Tilset, M.; Ystenes, M. Springer-Verlag Berlin **2001**, p. 3.

62. Siegbahn, P. E. M. *Adv. Chem. Phys.* **1996**, *93*, 333.

63. (a) Linnolahti, M. *Doctoral Dissertation: Correlations Between Ligand Structure and Polymerisation Activity of Zirconocene Catalysts Studied by ab-initio Hartree–Fock Method*, University of Joensuu, **2001**. (b) Linnolahti, M.; Hirva, P.; Pakkanen, T. A. *J. Comput. Chem.* **2001**, *22*, 51.

64. Results of a computational study on Cp_2MX_2 complexes by the extended Hückel molecular orbital method (Lauher, J. W.; Hoffmann, R. J. *Am. Chem. Soc.* **1976**, *98*, 1729) agree remarkably well with results of a more recent study

by the Fenske–Hall SCF method (Zhu, L.; Kostic, N. M. *J. Organomet. Chem.* **1987**, *335*, 395.)

65. Bianconi, A.; Incoccia, L. and Stipcich, S. (Eds.) EXAFS and Near Edge Structure, Springer, Berlin, **1983**.

66. See, for example, the following review and references therein: Resconi, L.; Cavallo, L.; Fait, A.; Piemontesi, F. *Chem. Rev.* **2000**, *100*, 1253.

67. (a) Piccolrovazzi, N.; Pino, P.; Consiglio, G.; Sironi, A.; Moret, M. *Organometallics* **1990**, *9*, 3098. (b) Henrici–Olivé, G.; Olivé, S. *Angew. Chem.* **1971**, *83*, 121. (c) Mäkelä, N. I. *Licentiate thesis: Effect of Structure Manipulation on the Electronic Properties of bis(cyclopentadienyl) and bis(indenyl) Zirconium (IV) Complexes*. University of Helsinki, **2001**.

68. Unpublished results by the author.

69. Hunter, W. E.; Hrncir, D. C.; Bynum, R. V.; Penttila, R. A.; Atwood, J. L. *Organometallics* **1983**, *2*, 750.

70. Repo, T.; Klinga, M.; Mutikainen, I.; Su, Y.; Leskelä, M.; Polamo, M. *Acta Crystallogr., Sect. C.* **1995**, *51*, 565.

71. Herrmann, W. A.; Rohrmann, J.; Herdtweck, E.; Spaleck, W.; Winter, A. *Angew. Chem., Int. Ed. Engl.* **1989**, *28*, 1511.

72. Zachmanoglou, G. E.; Docrat, A.; Bridgewater, B. M.; Parkin, G.; Brandow, C. G.; Bercaw, J. E.; Jardine, C. N.; Lyall, M.; Green, J. C.; Keister, J. B. *J. Am. Chem. Soc.* **2002**, *124*, 9525.

73. Linnolahti, M.; Pakkanen, T. A.; Leino, R.; Luttikhedde, H.; Wilén, C-E.; Näsman, J. H. *Eur. J. Inorg. Chem.*, **2001**, 2033.

74. Coevoet, D.; Cramail, H.; Deffieux, A.; Mladenov, C.; Pedeutour, J. N.; Peruch, F. *Polym. Int.* **1999**, *48*, 257

75. Marks, T. J.; Stevens, J. C. Eds. *Topics in Catalysis*, Baltzer, Amsterdam, **1999**, Vol. 7, pp. 23–36.

76. Tait, P. J. T.; Monteiro, M. G.; Yang, M.; Richardson, J. L. *Proceedings of MetCon **1996***, Houston, Texas.

77. Chien, J. C. W.; He, D. *J. Polym. Sci., Polym. Chem.* **1991**, *29*, 1603.

78. Patchornik, A.; Kraus, M. A.; *J. Am. Chem. Soc*. **1970**, *92*, 7587.

79. (a) Jezequel, M.; Dufayd, V.; Ruiz-Garzia, J.; Carrillo-Hermosilla, F.; Neugebauer, U.; Niccolai, G; Lefebvre, F.; Bayard, F.; Corker, J.; Fiddy, S.; Evans, J.; Broyer, J.; Malinge, J.; Basset,J. *J. Am. Chem. Soc*. **2001**, *123*, 3520. (b) Kröger-Laukkanen, M.; Peussa, M.; Leskelä, M.; Niinistö, L. *Appl. Surf. Sci.* **2001**, *183*, 290. (c) Uusitalo, A-M; Pakkanen, T. T.; Iskola, E. I. *J. Mol. Catal. A: Chem.* **2002**, *177*, 179.

80. (a) Dos Santos, J. H. Z.; Krug, C.; da Rosa, M. B.; Stedile, F. C.; Dupont, J.; Forte, M. C. *J. Mol. Catal. A: Chem.* **1999**, *139*, 199. (b) Stedile, F. C.; Dos Santos, J. H. Z. *Phys. Stat. Sol. (a)* **1999**, *173*, 123.

81. Atiqullah, M.; Faiz, M.; Akhtar, M. N.; Salim, M. A.; Ahmed, S.; Khan, J. H. *Surf. Interface Anal.* **1999,** *27*, 728.

82. O'Brien, S.; Tudor, J.; Maschmeyer, T.; O'Hare, D. *Chem. Commun.* **1997,** 1905.

83. Haag, M. C.; Krug, C.; Dupont, J.; de Gallant, G. B.; dos Santos, J. H. Z.; Uozumi, T.; Sano, T.; Soga, K. *J. Mol. Catal. A: Chem.* **2001**, *169*, 275.

84. (a) Sacchi, M. C.; Zucchi, D.; Tritto, I.; Locatelli, P.; Dall'Occo, T. *Macromol. Rapid Commun.* **1995**, *16*, 581. (b) Kaminsky, W.; Renner, F. *Macromol. Rapid Commun*. **1993,** *14*, 239.

85. Our test polymerisation studies show that (*n*-BuCp)2HfCl2 activated with MAO and supported on silica has roughly 2/3 of the activity of the corresponding zirconocene complex. The same conclusion was drawn in Mallin, D. T.; Rausch, M. D.; Chien, J. C. W. *Polym. Bull.* **1988**, *20*, 421.

86. Unpublished results. Complex 6 is deactivated by heat, while complexes 16 and 17 show higher polymerisation activities when heated.

87. Kallio, K.; Wartmann, A.; Reichert, K-H. *Macromol. Rapid Commun.* **2002**, *23*, 187.

88. Kallio, K.; Wartmann, A.; Reichert, K-H. *Macromol. Rapid Commun.* **2001**, *22*, 1334.

89. According to the DSC and FTIR measurements the side branch and end-group structures of the PE produced with and without O_2 in light are very similar.